

Latent Model Extreme Value Index Estimation

Joni Virta*

University of Turku

Aalto University School of Science

and

Niko Lietzén

Aalto University School of Science

and

Lauri Viitasaari

Aalto University School of Business

and

Pauliina Ilmonen

Aalto University School of Science

November 1, 2021

Abstract

We propose a novel strategy for multivariate extreme value index estimation. In applications such as finance, volatility and risk present in the components of a multivariate time series are often driven by the same underlying factors, such as the subprime crisis in the US. To estimate the latent risk, we apply a two-stage procedure. First, a set of

*Joni Virta gratefully acknowledges the financial support from the Academy of Finland (Grant 321883). Niko Lietzén gratefully acknowledges the financial support from the Emil Aaltonen Foundation (Grant 190135 N). All authors acknowledge the computational resources provided by the Aalto Science-IT project.

independent latent series is estimated using a method of latent variable analysis. Then, univariate risk measures are estimated individually for the latent series to assess their contribution to the overall risk. As our main theoretical contribution, we derive conditions under which the effect of the first step to the asymptotic behavior of the risk estimators is negligible. Simulations demonstrate the theory under both i.i.d. and dependent data, and an application into financial data illustrates the usefulness of the method in extracting joint sources of risk in practice.

Keywords: Blind source separation, Hill estimator, independent component analysis, moment estimator, tail index

1 Introduction

Let $\mathbf{x}_1, \dots, \mathbf{x}_n$ be a sample of p -variate random vectors with possibly dependent distributions. For each observation, we assume the instantaneous latent variable model,

$$\mathbf{x}_i = f(\mathbf{z}_i), \quad i = 1, \dots, n, \quad (1)$$

where the latent p -variate random vectors $\mathbf{z}_1, \dots, \mathbf{z}_n$ are assumed to have independent components in the sense that the k th component z_{ik} of \mathbf{z}_i is independent of the l th component z_{jl} of \mathbf{z}_l , for all i, j and $k \neq l$. Furthermore, we assume $f : \mathbb{R}^p \rightarrow \mathbb{R}^p$ is a deterministic function that is smooth and bijective. Note that while no explicit noise term is present in (1), the general formulation still captures noisy latent models as well, as one or several of the p latent components can represent noise which is then combined with the other components (signals) by the function f in a desired manner (additively, multiplicatively etc.).

The model (1) can be considered as a very general form of *independent component analysis* and has applications in numerous fields such as in telecommunications, psychometrics, economics and finance (Comon and Jutten, 2010; Hyvärinen and Oja, 2000). The model provides a powerful alternative to standard multivariate modelling schemes as, after having estimated the latent vectors, the independence of their components implies that all subsequent modeling can be done univariately. This structural simplification leads to both smaller number of parameters to estimate and simplified interpretations for the components as no interactions between the series need to be acknowledged.

In this paper we focus on estimating the tail behaviour of the latent variables in the model (1), evaluated through the *extreme value indices* of the corresponding distributions (De Haan and Ferreira, 2007). This is a natural goal to pursue in many financial and signal processing applications as the heaviness of the tails of a distribution is an indicator of an unstable and risky signal. For example, the independent component model has been applied in cashflow analysis and prediction of financial time series data (Kiviluoto and Oja, 1998; Lu et al., 2009; Yang and Yi, 2005), and in this context assessing the tail behaviour of the obtained independent components could help identify common sources of financial risk. Similarly, the evaluation of the extreme behaviour of latent components could help identify the sources

of abnormalities in applications such as biomedical imaging (Roberts, 2000) or maritime vessel track analysis (Smith et al., 2012).

This objective can be reached in two steps. First, we estimate a mapping \hat{f}^{-1} such that $\hat{f}^{-1}(\mathbf{x})$ equals the latent components up to order and scales (in latent component analysis, the order and scales of the latent components are usually neither of interest nor identifiable, see, e.g., Tong et al. (1991)). Especially under linear f , numerous techniques for obtaining consistent estimators under various types of data exist, see Section 4 for examples. Second, after having obtained the sample estimates $\hat{f}^{-1}(\mathbf{x}_1), \dots, \hat{f}^{-1}(\mathbf{x}_n)$ of the latent vectors, we use one of the several univariate extreme value index estimators presented in the literature (De Haan and Ferreira, 2007) to assess the extreme behavior of the individual, now independent, components.

Note that, in contrast to the above, the standard approach in multivariate extreme value theory is to assess the extreme behaviour component-wise for the observed multivariate signal itself (De Haan and Ferreira, 2007). Approaches which in some way acknowledge the multivariate structure of the data have been proposed only recently, and they include considering convex combinations of the component-wise estimators (Dematteo and Cl  men  on, 2016; Kim and Lee, 2017), extreme risk region estimation (Cai et al., 2011), and estimating the extreme value index of the generating variate of an underlying elliptical model (Dominicy et al., 2017; Heikkil   et al., 2019). However, these methods either involve complicated estimation or require strict distributional assumptions, making them less than ideal in practice. In comparison, our proposed two-step procedure is straightforward to apply and takes the multivariate form of the data into account in a natural way. Moreover, the associated latent variable model is flexible, allowing different tail behaviors for the underlying independent components. The only structural assumption we make is that the observed variables are generated by a set of independent factors.

1.1 Scope and structure of the paper

Of the two steps of our proposed method, we are primarily interested in the latter. That is, we focus on assessing the extreme behavior of the individual components in the independent component model (1). Throughout the article, we assume that there exists an estimator \hat{f}^{-1} with the asymptotic

linearization

$$\hat{\mathbf{z}}_i := \hat{f}^{-1}(\mathbf{x}_i) = \mathbf{z}_i + \hat{\mathbf{H}}\mathbf{z}_i + \hat{\mathbf{r}}, \quad (2)$$

where the $p \times p$ -matrix $\hat{\mathbf{H}} = \mathcal{O}_p(c_n^{-1})$ and the p -vector $\hat{\mathbf{r}} = \mathcal{O}_p(c_n^{-1})$ for some rate c_n . Here $\mathcal{O}_p(c_n^{-1})$ denotes the element-wise “convergence rate” in probability. For a precise definition, see Section 3. The form (2) is very general and encompasses many popular estimators \hat{f}^{-1} in the independent component analysis and blind source separation literature, see Section 4 for examples. Assuming for now that an estimator \hat{f}^{-1} exists in the sense of (2), our main objective is to estimate the extreme value indices of the components of the latent variables using $\hat{\mathbf{z}}_i$ as a proxy for \mathbf{z}_i , and to show that this approximation incurs no loss in asymptotic efficiency under a suitable set of assumptions.

A further complicating factor is that latent variable models such as (1) are well-known for not having fixed signs or scales for the latent components. That is, the vector \mathbf{z}_i on the right-hand side of (2) actually corresponds in many models to the true latent vectors only up to the signs and scales of its components. In the standard usage of latent variable modelling this is most often acceptable, as our interest lies commonly not in the signs, but in the shapes of the distributions of the latent variables. Similarly, in the present context, the scale of the components is irrelevant as most commonly applied extreme value index estimators are scale-invariant. However, as risk is estimated from the tails of the components, knowing in which of the tails we are in is for our purposes of paramount importance, and we need a way of identifying the correct tail. A simple, but restrictive, solution would be to require that all the latent components have symmetric distributions. Instead, we choose to assess the extreme behaviour of, not the latent components, but their absolute values. This rids us of the sign indeterminacy by “stacking” the two tails on top of each other. Since the absolute value inherits its tail behaviour from the heavier of the two tails, this approach has the interpretation of us always looking at the heavier of the two tails. Moreover, as heavier tails correspond to larger risk, the use of absolute values can be seen as a conservative approach to tail behaviour estimation.

The rest of the paper is organized as follows: Preliminaries on extreme value theory along with the popular extreme value index estimators, the Hill estimator and the moment estimator, are reviewed in Section 2. These extreme value index estimators are known to be consistent and asymptotically

normal under mild technical conditions. In Section 3, we derive sufficient conditions ensuring that the asymptotic properties of the extreme value estimators are preserved when estimated using the proxy sample $\hat{f}^{-1}(\mathbf{x}_i)$. In Section 4, we consider two example cases of the general framework and discuss the particular assumptions needed to achieve the limiting results for the corresponding proxy samples. In Section 5, we present a large simulation study and a real data application is considered in Section 6. All the proofs are postponed to the supplementary appendix, along with a supplementary simulation study and additional details concerning the real data example.

2 Preliminaries on extreme value theory

In the following we provide a brief introduction to the topics in univariate extreme value theory that are most relevant to our objectives. See De Haan and Ferreira (2007) and the references therein for more information.

Consider an i.i.d. random sample $\mathbf{y} = (y_1, \dots, y_n)$ from a univariate distribution F and the sample maximum $M_n = \max_{1 \leq i \leq n} y_i$. If there exists sequences of constants $a_n > 0$ and b_n such that $a_n M_n + b_n$ has a limiting distribution G , we say that G is the *extreme value distribution* of F . One of the fundamental results in extreme value theory is the Fisher-Tippett-Gnedenko theorem which identifies the class of distributions G .

Theorem 1 (Fisher-Tippett-Gnedenko). *The class of extreme value distributions is $G_\gamma(ax + b)$ with $a > 0$ and $b \in \mathbb{R}$, where*

$$G_\gamma(x) = \exp\left(- (1 + \gamma x)^{-1/\gamma}\right), \quad 1 + \gamma x > 0,$$

with $\gamma \in \mathbb{R}$ and where for $\gamma = 0$ the right-hand side is interpreted as $\exp(-e^{-x})$.

According to Theorem 1, the family of possible extreme value distributions has a remarkably simple form, parametrized by a single real number γ . If G_γ is the extreme value distribution of F , the distribution F is said to be in the *domain of attraction* of G_γ , and we write $F \in G_\gamma$. The parameter γ is said to be the *extreme value index* of F . The parameter γ measures the thickness of the (right) tail of F and knowing its value leads to a complete characterization of the asymptotic tail behavior of F , allowing extrapolating probabilities beyond the observed dataset. Thus γ is a key ingredient in risk assessment.

It is widely accepted that distributions are divided into heavy and light tailed ones based on the sign of γ . More precisely, for $\gamma > 0$, the distributions $F \in G_\gamma$ are called *heavy tailed* and belonging to the domain of attraction of the *Frechet* distribution. Similarly, if $\gamma < 0$ and $F \in G_\gamma$, then we say that F is *light tailed* and belongs to the domain of attraction of the *Weibull* distribution. Finally, if $F \in G_0$, then F belongs to the domain of attraction of the *Gumbel* distribution. This corresponds to the border case between light and heavy tails, and includes, e.g., the case of a normal distribution.

One of the most commonly applied classical estimators of the extreme value index, suitable for $\gamma > 0$, is the Hill estimator introduced in Hill (1975),

$$\hat{\gamma}_H(\mathbf{y}) = \frac{1}{k_n} \sum_{m=0}^{k_n-1} \log \frac{(\mathbf{y})_{(n-m,n)}}{(\mathbf{y})_{(n-k_n,n)}},$$

where $(\mathbf{y})_{(n,n)} \geq \dots \geq (\mathbf{y})_{(1,n)}$ are the order statistics of the sample \mathbf{y} , and $1 \leq k_n \leq n$ is a sequence of thresholds for the portion of observations that are considered to form the tail. Common choices for the threshold include, e.g., $k_n = \sqrt{n}$ and $k_n = \log(n)$.

Another well-known estimator, which in turn is valid for any value of γ , is the moment estimator introduced in Dekkers et al. (1989). As in the Hill estimator, set

$$M_n^{(j)}(\mathbf{y}) = \frac{1}{k_n} \sum_{m=0}^{k_n-1} \left(\log \frac{(\mathbf{y})_{(n-m,n)}}{(\mathbf{y})_{(n-k_n,n)}} \right)^j.$$

Here $j = 1, 2, \dots$ is given, and the Hill estimator corresponds to the choice $j = 1$. The moment estimator is based on the choices $j = 1, 2$ and is given by

$$\hat{\gamma}_M(\mathbf{y}) = M_n^{(1)}(\mathbf{y}) + 1 - \frac{1}{2} \left(1 - \frac{[M_n^{(1)}(\mathbf{y})]^2}{M_n^{(2)}(\mathbf{y})} \right)^{-1}.$$

In the next section, both the Hill estimator and the moment estimator are used to estimate the extreme value indices of the absolute values of the latent components in (1).

3 Extreme value index estimation for latent variables

Recall from Section 1 that we consider an estimated sample $\hat{\mathbf{z}}_1, \dots, \hat{\mathbf{z}}_n$ of the latent vectors $\mathbf{z}_1, \dots, \mathbf{z}_n$ satisfying

$$\hat{\mathbf{z}}_i = \mathbf{z}_i + \hat{\mathbf{H}}\mathbf{z}_i + \hat{\mathbf{r}}, \quad (3)$$

where the $p \times p$ -matrix $\hat{\mathbf{H}} = \mathcal{O}_p(c_n^{-1})$, and the p -vector $\hat{\mathbf{r}} = \mathcal{O}_p(c_n^{-1})$ for some rate c_n . Here, and throughout the paper, the notation $X_n = \mathcal{O}_p(g_n)$ is used to denote that the family of random variables $g_n^{-1}X_n$ is uniformly tight. Similarly, we use other Landau notation, such as $o(1)$ to indicate convergence towards zero. With \rightarrow_p , we denote convergence in probability, and with \rightsquigarrow , we indicate weak convergence, i.e., convergence in distribution.

Recall further, that the idea underlying the model (3) is that the vector $\hat{\mathbf{z}}_i$ is an estimate of \mathbf{z}_i obtained by solving some latent variable model. However, for the following results to hold, simply having the form (3) is sufficient, regardless of how it originated.

A common assumption in extreme value literature as well as in the latent variable literature is to assume that each component z_i^k of the true non-observable signals \mathbf{z}_i is strictly stationary, and has a univariate marginal F_k , i.e., each observation z_i^k has marginal distribution F_k , for all i . One typical example is the case where observations are i.i.d., with components drawn from different distributions. Another typical example is the case where the components z_i^k form different stationary series with marginals F_k . However, while our main examples arise from stationary series falling into the above setting, our main results do not even require stationarity of the components z_i^k (although it might be difficult to interpret the estimated extreme value index if the one dimensional marginals are not equal).

It is also customary in the field of extreme value theory to assume that marginals do not have point-mass at zero. In our case, this ensures that our logarithm-based estimators are well-defined. That is, in the general non-stationary case, we assume that, for each component $k = 1, 2, \dots, p$, we have

$$\liminf_{\delta \rightarrow 0} \mathbb{P} \left(|z_i^k| \geq \delta \right) = 1. \quad (4)$$

In the sequel, (4) is always assumed, even if it is not explicitly stated. Note that (4) is a natural assumption and not very restrictive. First of all, (4)

implies that $\mathbb{P}(z_i^k = 0) = 0$ for all i and k . Moreover, in the case of equal marginals, (4) is equivalent to $\mathbb{P}(z_i^k = 0) = 0$. In the general case, (4) excludes also the situations where the observations come from a sequence of distributions $F_{i,k}$ that approach a distribution having point mass at zero.

In the sequel, the notation $|\mathbf{z}^k|$ refers to the sample $|z_{1k}|, \dots, |z_{nk}|$ of the absolute values of the k th latent series and $|\mathbf{z}^k|_{(m,n)}$ denotes the m th largest element of $|\mathbf{z}^k|$.

Throughout the article, we make the following assumption.

Assumption 1. *For all $k = 1, \dots, p$, there exists deterministic sequences a_{nk}, b_{nk} for which the k th component z_{ik} of \mathbf{z}_i satisfies*

$$\frac{|\mathbf{z}^k|_{(n,n)} - b_{nk}}{a_{nk}} = \mathcal{O}_p(1).$$

We stress that Assumption 1 is very relaxed, and in the extreme value theory literature it is usually taken as granted, without explicitly stating it. Indeed, if the observations are independent with a distribution function F , then Assumption 1 follows immediately whenever $F \in G_\gamma$, i.e., F is in the domain of attraction of some extreme value distribution G_γ . Thus, in the case of independent observations, discussing the extreme value index γ without Assumption 1 is not sensible. More generally, Assumption 1 follows immediately whenever $a_{nk}^{-1} (|\mathbf{z}^k|_{(n,n)} - b_{nk})$ converges towards some distribution. For example, Assumption 1 is trivially valid even in the totally degenerate case $z_{ik} = z_k$, for all i .

The main contribution of this article is the derivation of sufficient conditions under which the asymptotic properties of the Hill and moment estimators are preserved under Model (3). Intuitively, one would expect that these asymptotic properties remain the same, provided that c_n^{-1} vanishes rapidly enough to compensate the growth of the sample maximum of the heaviest component. Theorem 2 and Theorem 3 below contain the precise statements of this heuristic argument. In the sequel, we use the notation $g_{nk} = \max\{a_{nk}, b_{nk}\}$.

Theorem 2. *Let Assumption 1 hold and assume that,*

$$\frac{\max_\ell \{g_{n\ell}\}}{c_n} = o(1). \tag{5}$$

Let $k \in \{1, \dots, p\}$ be fixed and let C_H and C_M be arbitrary constants.

- i) If $\hat{\gamma}_H(|\mathbf{z}^k|) \rightarrow_p C_H$, then $\hat{\gamma}_H(|\hat{\mathbf{z}}^k|) \rightarrow_p C_H$.
- ii) If $\hat{\gamma}_H(|\mathbf{z}^k|) \rightarrow_p C_H$, $\frac{\max_{\ell}\{g_{n\ell}\}}{c_n \hat{\gamma}_H(|\mathbf{z}^k|)} \rightarrow_p 0$ and $\hat{\gamma}_M(|\mathbf{z}^k|) \rightarrow_p C_M$, then $\hat{\gamma}_M(|\hat{\mathbf{z}}^k|) \rightarrow_p C_M$.

Note that in the above result it is not required that C_H and C_M are the correct extreme value indices — any constants suffice. Indeed, the part i) of Theorem 2 simply states that whenever the Hill estimator based on the "true" latent signals converges towards some constant, then the Hill estimator based on the estimated latent signals converges towards the same constant. The reason behind our formulation is that usually, as is the case for independent observations, the Hill estimator converges towards $\max(0, \gamma)$, see De Haan and Ferreira (2007), pp. 101. In other words, the Hill estimator vanishes for distributions that are not heavy tailed. For such distributions, one can then apply the moment estimator. Part ii) of Theorem 2 says that whenever both, the Hill estimator and the moment estimator based on the true latent signals $|\mathbf{z}^k|$, converge towards any constants, then the Hill and the moment estimator based on the estimated latent signals converge towards the same constants. As in most cases the Hill estimator converges towards $\max(0, \gamma)$, and does not explode, part ii) of Theorem 2 implies that asymptotic properties of the moment estimator are inherited to the estimated model as well. The extra condition in part ii) concerns the case when the Hill estimator converges towards zero, $C_H = 0$, and ensures that this convergence is not too rapid in comparison to the growth of the heaviest tail. In many cases of interest, the convergence rate of the Hill estimator is $\sqrt{k_n}$. This leads to the same condition as in Theorem 3, and can be achieved by a suitable choice of k_n . Finally, we stress that an examination of the proof of Theorem 2 reveals that the item ii) is valid as long as the Hill estimator does not tend to infinity. Thus one can safely apply the moment estimator for light tailed distributions under Model (3).

In order to gain better understanding on the behavior of the estimators, we next consider their limiting distributions.

Theorem 3. *Let Assumption 1 hold and assume that,*

$$\frac{\sqrt{k_n} \max_{\ell}\{g_{n\ell}\}}{c_n} = o(1). \quad (6)$$

Let $k \in \{1, \dots, p\}$ be fixed and let $C_H, C_M, \mu_H, \mu_M, \sigma_H$, and σ_M be arbitrary constants.

i) If $\sqrt{k_n} (\hat{\gamma}_H(|\mathbf{z}^k|) - C_H) \rightsquigarrow \mathcal{N}(\mu_H, \sigma_H^2)$, then

$$\sqrt{k_n} (\hat{\gamma}_H(|\hat{\mathbf{z}}^k|) - C_H) \rightsquigarrow \mathcal{N}(\mu_H, \sigma_H^2).$$

ii) If $\hat{\gamma}_H(|\mathbf{z}^k|) \rightarrow_p C_H$, $\frac{\sqrt{k_n} \max_\ell \{g_{n\ell}\}}{c_n \hat{\gamma}_H(|\mathbf{z}^k|)} \rightarrow_p 0$, and $\sqrt{k_n} (\hat{\gamma}_M(|\mathbf{z}^k|) - C_M) \rightsquigarrow \mathcal{N}(\mu_M, \sigma_M^2)$, then

$$\sqrt{k_n} (\hat{\gamma}_M(|\hat{\mathbf{z}}^k|) - C_M) \rightsquigarrow \mathcal{N}(\mu_M, \sigma_M^2).$$

In the above result, the constants μ_H, μ_M, σ_H , and σ_M can be computed explicitly in most cases, their exact values depending on the so-called second order conditions. For details, we refer to De Haan and Ferreira (2007). We also remark that in our proof, we could easily replace the convergence rate $\sqrt{k_n}$ with some other rate, or the limiting normal distribution with some other distribution. The underlying reason for the above formulation is that we are not aware of any asymptotic results for extreme value index estimators where the rate is other than $\sqrt{k_n}$ or where the limiting distribution is not normal.

We end this section by discussing the strictness of the key conditions $\max_\ell \{g_{n\ell}\} = o(c_n)$ and $\sqrt{k_n} \max_\ell \{g_{n\ell}\} = o(c_n)$. These conditions state that the convergence rate c_n of the estimated latent sample to the true latent sample must be sufficiently fast compared both to $\sqrt{k_n}$, the square root of the tail threshold, and to $\max_\ell \{g_{n\ell}\}$, the heaviness of the heaviest of the latent components. Moreover, the rate k_n can be seen as a type of a tuning parameter. Choosing a faster growing k_n will make the Hill estimator converge more rapidly, but it will, at the same time, limit the range of distributions whose extreme value indices we can estimate in the first place, and vice versa.

To shed further light on these conditions, we consider an example. Assume that there exists at least one latent component belonging to the domain of attraction of the Fréchet distribution, i.e., $\max_\ell \{g_{n\ell}\} = \mathcal{O}(n^\gamma)$ for some $\gamma > 0$ (cf. Lemma 1 in the supplementary Appendix A). Now, letting $k_n = n^\alpha$ for some $\alpha > 0$ and under the standard rate $c_n = \sqrt{n}$, we end up with the restriction $\gamma < \frac{1}{2}(1 - \alpha)$. Hence, putting the tail threshold k_n sufficiently small, we see that extreme value index estimation is feasible as long as the heaviest Fréchet component among the latent variables has its extreme value index smaller than $1/2$, that is, all latent components have finite variance. Heavier

components, i.e., ones without second moments, can be captured through estimators which yield faster convergence rates c_n than the usual \sqrt{n} for the model estimation. Conversely, if the convergence rate c_n is slower than the usual \sqrt{n} (see, e.g., Lietzén et al. (2020)), then c_n might not be sufficient to compensate too heavy tails, and, e.g., assumptions on the existence of higher moments are required.

4 Example models

In this section, we illustrate the applicability of our main results by considering two popular example models: stationary independent component model and stationary second order source separation model. For simplicity, we only consider the Hill estimator, although the following analysis could be easily extended for the moment estimator as well (see Remark 1). Throughout, we assume that the heaviest component has index $\gamma > 0$, often implying that $\max_{\ell} \{g_{n\ell}\} = \mathcal{O}(n^\gamma)$, see the examples below. As the rate $c_n = \sqrt{n}$ is the best possible that one can usually expect, we also assume $\gamma < \frac{1}{2}$. This ensures the square integrability of all of our random variables, which is also a minimum requirement for (3) to hold for the standard estimation procedures in our example models.

Let now $k \in \{1, \dots, p\}$ be fixed. We illustrate our results in cases where both Theorem 2 and Theorem 3 are applicable. Thus, in order to obtain limiting normality for the Hill estimator $\hat{\gamma}_H(|\mathbf{z}^k|)$ based on the true values $|\mathbf{z}^k|$, we impose a second order condition for the marginal distribution F of $|z^k|$. The distribution F is called *second order regularly varying* (with index γ) if there exists a positive or negative function A with the property $\lim_{t \rightarrow \infty} A(t) = 0$ such that, for all $x > 0$,

$$\lim_{t \rightarrow \infty} \frac{\frac{U(tx)}{U(t)} - x^\gamma}{A(t)} = x^\gamma \frac{x^\rho - 1}{\rho}, \quad (7)$$

holds for some real number $\rho \leq 0$. Here the function U is given by

$$U = \left(\frac{1}{1 - F} \right)^\leftarrow,$$

where $^\leftarrow$ denotes the left-continuous (pseudo-)inverse function. Then, in the case of independent observations, the limiting normality,

$$\sqrt{k_n} \left(\hat{\gamma}_H(|\mathbf{z}^k|) - \gamma \right) \rightsquigarrow \mathcal{N} \left(\frac{\lambda}{1 - \rho}, \sigma^2 \right), \quad (8)$$

holds, provided that $\lim_{n \rightarrow \infty} \sqrt{k_n} A\left(\frac{n}{k_n}\right) = \lambda \in \mathbb{R}$. This leads to an upper bound on the rate at which k_n can grow. Similarly, conditions of Theorems 2 and 3 give upper bounds for the rate at which k_n can grow. Thus, we can obtain limiting normality (and consistency) by choosing a not-too-rapidly growing sequence k_n , at the cost of a slower rate of convergence. For details on the limiting normality of the Hill estimator in the case of i.i.d. observations, see De Haan and Ferreira (2007), and in the case of stationary dependent observations, see De Haan et al. (2016) and the references therein.

4.1 Independent component model

In independent component analysis (ICA) the observed p -vectors $\mathbf{x}_1, \dots, \mathbf{x}_n$ are assumed to be a random sample from the independent component (IC) model,

$$\mathbf{x} = \mathbf{\Omega}\mathbf{z} + \boldsymbol{\mu}, \quad (9)$$

where the latent p -vector \mathbf{z} has independent components, $\mathbf{\Omega} \in \mathbb{R}^{p \times p}$ is invertible and $\boldsymbol{\mu} \in \mathbb{R}^p$ is a location parameter (Hyvärinen and Oja, 2000). The objective in ICA is find an unmixing matrix $\mathbf{\Gamma} \in \mathbb{R}^{p \times p}$, such that $\mathbf{\Gamma}\mathbf{x}$ has independent components. Standard theory then shows that if at most one of the ICs is Gaussian, any such solution coincides with \mathbf{z} up to scaling, order and signs of the components. The scales can be fixed by second order standardisation of \mathbf{z} . This guarantees that all the solutions are of the form $\mathbf{\Gamma} = \mathbf{P}\mathbf{J}\mathbf{\Omega}^{-1}$ where $\mathbf{P} \in \mathbb{R}^{p \times p}$ is a permutation matrix and $\mathbf{J} \in \mathbb{R}^{p \times p}$ is a sign-change matrix (diagonal matrix with diagonal entries equal to ± 1). In our approach in assessing extreme behaviour, the sign ambiguity is of no concern, as we consider the absolute values of the source components. Moreover, the order of the components is irrelevant, if one is interested in modelling the tail index of the component with the highest risk.

Numerous estimators $\hat{\mathbf{\Gamma}}$ of the unmixing matrix have been proposed and under suitable assumptions and standardisations, most estimators converge to $\mathbf{\Omega}^{-1}$ at some rate c_n ,

$$c_n \left(\hat{\mathbf{\Gamma}}\mathbf{\Omega} - \mathbf{I}_p \right) = \mathcal{O}_p(1). \quad (10)$$

Typically, in the context of i.i.d. observations, we have $c_n = \sqrt{n}$. See Miettinen et al. (2015) for several examples including FastICA (Hyvärinen, 1999),

fourth order blind identification (FOBI) (Cardoso, 1989), and joint approximate diagonalization of eigenmatrices (JADE) (Cardoso and Souloumiac, 1993). Also the ICA-estimators based on the simultaneous diagonalization of two symmetrized scatter matrices (Oja et al., 2006; Nordhausen et al., 2008) can be shown to have the rate \sqrt{n} , assuming that the applied symmetrized scatter matrices have the same convergence rate.

Assuming that $\hat{\Gamma}$ is of the form (10), the estimated latent vectors can be written as

$$\hat{\mathbf{z}}_i = \hat{\Gamma}(\mathbf{x}_i - \bar{\mathbf{x}}) = \hat{\Gamma}\Omega(\mathbf{z}_i - \bar{\mathbf{z}}) = \mathbf{z}_i + (\hat{\Gamma}\Omega - \mathbf{I}_p)\mathbf{z}_i - \hat{\Gamma}\Omega\bar{\mathbf{z}}.$$

Writing now $\hat{\mathbf{H}} := \hat{\Gamma}\Omega - \mathbf{I}_p$ and $\hat{\mathbf{r}} := -\hat{\Gamma}\Omega\bar{\mathbf{z}}$, we observe that we have arrived to the form (3). By the assumption that $\max_{\ell}\{g_{n\ell}\} = \mathcal{O}(n^{\gamma})$ with $\gamma < \frac{1}{2}$, we observe that (5) is automatically valid, and (6) is valid for suitably chosen sequence k_n . We stress that $\gamma < \frac{1}{2}$ guarantees the existence of second moments, while usually standard ICA methods operate on higher-order information making even stronger moment assumptions. For example, the \sqrt{n} -consistency for FOBI requires the existence of finite eighth moments of the latent variables (Ilmonen et al., 2010). By using squared FastICA with the hyperbolic tangent (Miettinen et al., 2017) as the ICA-estimator, one can reduce the order of the required moments to four. Finally, we stress that under independent observations drawn from a second order regular varying heavy tailed distribution, the Hill estimator $\hat{\gamma}_H(|\mathbf{z}^k|)$ is consistent and asymptotically normal (see De Haan and Ferreira (2007)), and while different technical assumptions are required for the classical ICA-estimators, none of them interfere with our assumption that guarantees the consistency and limiting normality of the Hill estimator. Thus, as a conclusion, we can safely apply Theorem 2 and Theorem 3.

Remark 1. *In the above discussions we have considered only the Hill estimator. However, applying Theorem 2 or Theorem 3 for the moment estimator in the ICA-context is straightforward. Indeed, under second order regularly varying tails and independence, the Hill estimator always converges to $\max(0, \gamma)$, and the moment estimator is both consistent and asymptotically normal. Thus it suffices to check the extra condition $\frac{\sqrt{k_n} \max_{\ell}\{g_{n\ell}\}}{c_n \hat{\gamma}_H(|\mathbf{z}^k|)} \rightarrow_p 0$. However, even if $\gamma \leq 0$ we have $\sqrt{k_n} \hat{\gamma}_H(|\mathbf{z}^k|) \rightsquigarrow \mathcal{N}(\mu_H, \sigma_H^2)$, and thus it suffices to choose the sequence k_n such that $\frac{k_n \max_{\ell}\{g_{n\ell}\}}{c_n} = o(1)$.*

4.2 Second order source separation model

Our second example moves to the realm of signal processing and blind source separation (BSS). Like the IC model, also the second order BSS model is linear and based on the general location-scatter model. In the model, the observed run $\mathbf{x}_1, \dots, \mathbf{x}_n$ of a stationary p -variate time series is assumed to have the instantaneous latent representation,

$$\mathbf{x}_i = \mathbf{\Omega} \mathbf{z}_i + \boldsymbol{\mu}, \quad i \in \{1, \dots, n\}, \quad (11)$$

where the latent p -variate time series \mathbf{z}_i is stationary and has standardized uncorrelated components, and $\mathbf{\Omega} \in \mathbb{R}^{p \times p}$ is of full rank. The location $\boldsymbol{\mu} \in \mathbb{R}^p$ is (by stationarity) trivial to estimate by using a standard average estimator, which provides a consistent estimator if the system is ergodic. Thus, for the sake of simplicity, it will be omitted in the following. Note also that the non-identifiability of signs and order holds in the BSS model as well. However, for our purposes this does not matter due to the reasons explained in Subsection 4.1.

One standard approach to estimate \mathbf{z}_i is algorithm for multiple unknown signals extraction (AMUSE) (Tong et al., 1990) where the autocovariance matrices $\boldsymbol{\Sigma}_\tau(\mathbf{x}_i) = \mathbb{E}(\mathbf{x}_i \mathbf{x}_{i+\tau}^\top)$ for $\tau \in \{0, \tau_0\}$ are diagonalised simultaneously. An extension of AMUSE that is less sensitive to the choice of τ_0 is the second order blind identification (SOBI) (Belouchrani et al., 1997) algorithm where the autocovariance matrices $\boldsymbol{\Sigma}_\tau(\mathbf{x}_i) = \mathbb{E}(\mathbf{x}_i \mathbf{x}_{i+\tau}^\top)$ over a chosen set of lags $\mathcal{T} = \{\tau_1, \dots, \tau_{|\mathcal{T}|}\}$ are jointly diagonalized. As in the IC-model, one would expect that the algorithm provides a consistent estimator $\hat{\mathbf{\Gamma}}$ with some rate c_n :

$$c_n \left(\hat{\mathbf{\Gamma}} \mathbf{\Omega} - \mathbf{I}_p \right) = \mathcal{O}_p(1). \quad (12)$$

It turns out that (12) holds true whenever

$$c_n \left(\hat{\boldsymbol{\Sigma}}_\tau(\mathbf{x}_i) - \boldsymbol{\Sigma}_\tau(\mathbf{x}_i) \right) = \mathcal{O}_p(1), \quad \tau \in \mathcal{T}, \quad (13)$$

where $\hat{\boldsymbol{\Sigma}}_\tau(\mathbf{x}_i)$ denotes the estimator of the autocovariance matrix $\boldsymbol{\Sigma}_\tau(\mathbf{x}_i)$. The fact that (13) implies (12) is proved in the case of complex valued AMUSE in Lietzén et al. (2020) with general rate c_n , and in the case of real valued SOBI (and its variants) in Miettinen et al. (2016) for the rate $c_n = \sqrt{n}$. It is also straightforward to check that the arguments of Miettinen et al. (2016) apply with arbitrary rate function c_n . For examples with general rate c_n instead of the standard \sqrt{n} , we refer to Lietzén et al. (2020).

Equation (13) is the first key assumption on the rate of convergence for the autocovariance estimators, which on the other hand gives us our speed c_n . If c_n is non-standard, (5) gives us also the restriction $n^\gamma = o(c_n)$, limiting the possible values of γ . This can be seen as an interchange between moment assumptions and the speed at which the autocovariance estimators converge, as higher moments are required if the estimators converge slowly.

In order to make Theorem 3 applicable, we also require that the Hill estimator $\hat{\gamma}_H(|\mathbf{z}^k|)$ satisfies limiting normality (8). Compared to independent observations, the problem is much more subtle in the case of dependent sequences and one needs to pose extra assumptions in addition to the second order regularly varying condition (7). The extra assumptions are, roughly speaking, conditions that ensure the dependence to be weak enough so that the series "behaves" similarly as a series of independent observations. The precise definition of weak dependence or asymptotic independence varies in the literature. Usually asymptotic independence is encoded to mixing-conditions (for different notions of mixing-conditions and their relations, see the survey in Bradley (2005)). It is known (see, e.g., Drees (2000, 2003)) that (8) holds provided that $|\mathbf{z}^k|$ forms a β -mixing stationary sequence such that some minor additional regularity conditions are met (see, e.g., conditions (a)-(c) of De Haan et al. (2016)). In particular, all these conditions are satisfied for the following sequences:

- m -dependent process and AR(1)-process (Drees, 2003; Rootzén, 1995, 2009),
- AR(p)-processes and MA(∞)-processes (with suitable assumptions on the coefficients) (Drees, 2002; Resnick and Stărică, 1997),
- MA(q)-processes (Drees, 2002; Hsing, 1991; Rootzén, 1995, 2009),
- ARCH(1)-processes (Drees, 2002, 2003),
- GARCH-processes (Drees, 2000; Stărică, 1999).

We emphasize that the above examples form a very large and applicable class of processes. For details and more information on the above examples, see also De Haan et al. (2016).

We now turn back to extreme value index estimation under the BSS model. In order to apply Theorem 2 or Theorem 3, it suffices to make sure

that, for a given heavy tailed component $|\mathbf{z}^k|$, the above mentioned conditions guaranteeing the limiting normality (8) for the Hill estimator $\hat{\gamma}_H(|\mathbf{z}^k|)$ are satisfied. At the same time, one needs that (13) holds, with some rate c_n satisfying $n^\gamma = o(c_n)$. After that, it remains to choose k_n not increasing too rapidly so that (6) holds as well. We next explore the connection between the given assumptions. We first observe that conditions required to ensure (8) are solely on the dependence structure and distribution of the given component $|\mathbf{z}^k|$ of interest. At the same time, condition (13) considers the rate of convergence of autocovariance estimators for all components simultaneously. Note that β -mixing and assumptions (a)-(c) of De Haan et al. (2016) do not imply convergence of the autocovariance estimators (as the conditions do not even require existence of second moments). Conversely, convergence of the autocovariance estimators is related to the so-called ρ -mixing (see Bradley (2005) for precise definition) which does not imply β -mixing. Thus, even the convergence rate of the autocovariance estimator of the component $|\mathbf{z}^k|$ does not provide any information regarding the validity of conditions implying limiting normality (8) for the Hill estimator. This means that the assumptions do not contradict, and also that in practice, one has to verify (13) and the limiting normality of the Hill estimator separately.

Remark 2. *If all components are ρ -mixing, then the slowest decay of the ρ -mixing coefficients gives us an upper bound for c_n . Moreover, if one poses a stronger mode of mixing, ϕ -mixing, for the sequence $|\mathbf{z}^k|$, then (Bradley, 2005, p.112) the sequence is also both β - and ρ -mixing. For example, this is the case for m -dependent processes and GARCH-processes.*

5 Simulations

In this section, we illustrate the tail index estimation under the second order source separation model of Section 4.2 through a simulation study. Appendix B in the supplementary material presents a similar study for the independent component model in Section 4.1, with largely the same conclusions.

In this simulation study, we consider the \mathbb{R}^3 -process \mathbf{z} , where the components are n -length realizations, i.e., time series, of the independent stochastic processes in $\tilde{\mathbf{z}} = (\text{ARCH}(1), \text{D}^{(1)}, \text{D}^{(2)})^\top$. The first component of $\tilde{\mathbf{z}}$ is an ARCH(1)-process with the parameter vector $(\alpha_0, \alpha_1) = (1/4, (2^3 \sqrt{2/\pi})^{-2/5})$. At time t , the second and third components are defined as $\text{D}_t^{(1)} = (B_{t+1}^{(1)} - B_t^{(1)})^2 -$

1 and $D_t^{(2)} = (B_{t+1}^{(2)} - B_t^{(2)})^2 - 1$, where $B^{(1)}$ denotes a fractional Brownian motion (fBm) with Hurst parameter $3/4$ and $B^{(2)}$ denotes a fBm with Hurst parameter $4/5$, such that $B^{(1)}$ and $B^{(2)}$ are mutually independent. For a comprehensive study on fBm, see, e.g., Nualart (2006). Out of the three components, the ARCH(1) process has the largest theoretical extreme value index $1/5$. We considered the sample sizes $n \in \{300, 10^3, 10^4, 10^5, 10^6, 10^7\}$ and the threshold sequence k_n was chosen to be $k_n = \lfloor n^{1/4} \rfloor$. For each sample size, the simulation was iterated 2000 times.

As a preliminary step, the simulated observations $\tilde{\mathbf{z}}_i$ were centered. Here, the centered observations are denoted as \mathbf{z}_i . In every iteration $h \in \{1, \dots, 2000\}$, we applied, for all $i \in \{1, \dots, n\}$, the linear transformation $\mathbf{x}_i = \mathbf{\Omega}_h \mathbf{z}_i$, where the elements of the $\mathbb{R}^{3 \times 3}$ -matrix $\mathbf{\Omega}_h$ were simulated independently, and separately in every iteration, from the univariate uniform distribution $\text{unif}(-100, 100)$. We then applied the AMUSE unmixing procedure with lag $\tau = 1$ to the mixed time series, using the implementation contained in the R-package JADE (Miettinen et al., 2017). The existence of the limiting distribution of the AMUSE unmixing estimator requires finite fourth moments. Note that the ARCH(1) parameters α_0, α_1 are chosen such that the fourth moments exist for all components. We denote the absolute values of the AMUSE unmixed time series and the absolute values of the original centered time series as $|\hat{\mathbf{z}}|$ and $|\mathbf{z}|$, respectively.

Now, we have $\max_{\ell}(g_{n\ell}) = n^{-1/5}$, which corresponds to the ARCH(1) process. The $D^{(2)}$ process in the third component has the slowest rate of convergence, giving $c_n = n^{2/5}$, see Lietzén et al. (2020). Hereby, under our choice of $k_n = \lfloor n^{1/4} \rfloor$, we have that the assumptions required by Theorems 2 and 3 hold and, hence, for large sample sizes, the extreme value index estimates calculated from $|\hat{\mathbf{z}}|$ and $|\mathbf{z}|$ are expected to be close to each other.

We estimated the extreme value indices for every component from both $|\hat{\mathbf{z}}|$ and $|\mathbf{z}|$, using both the Hill estimator and the moment estimator. Note that both estimators produce three extreme value index estimates, one for each component. To capture the ARCH(1) component, we collected, in every simulation iteration, the largest of the three estimates, denoted in the following by $\hat{\gamma}(|\hat{\mathbf{z}}|)$ and $\hat{\gamma}(|\mathbf{z}|)$ (this induces a slight bias to the results which is, however, rendered negligible with increasing n). The histograms of $\hat{\gamma}(|\hat{\mathbf{z}}|)$ and $\hat{\gamma}(|\mathbf{z}|)$ for sample sizes $n = 300, 10^3, 10^4$ are shown in Figure 1, where the extreme value indices estimated from $|\hat{\mathbf{z}}|$ correspond to light blue colour, and the extreme value index estimates calculated from the original $|\mathbf{z}|$ correspond

to light red colour. Dark blue colour is used for the parts of the histograms that overlap and the dashed yellow vertical line represents the theoretical extreme value index value $\gamma = 1/5$. Values smaller than -2 are omitted from the figure; a total of 21 moment estimator estimates were smaller than -2 .

In Figure 1, already for the small sample size $n = 300$, the two histograms overlap significantly. Moreover, starting from $n = 1000$, the histograms are basically identical, showing that, as predicted by the theory, the effect of the BSS-step on the estimation of the extreme value indices is almost negligible. When comparing the Hill estimator and the moment estimator, Figure 1 indicates that the variance of the moment estimator is larger, when compared to the Hill estimator. In addition, the bias of the Hill estimator is visible in the histograms, see De Haan and Ferreira (2007), and seems to decrease as the sample size increases. The histograms corresponding to the sample sizes $10^5, 10^6$ and 10^7 have been omitted here, as they introduce no new information to the simulation study.

Figure 2 illustrates the absolute differences, scaled with $\sqrt{k_n}$, between the estimates calculated from $|\mathbf{z}|$ and $|\hat{\mathbf{z}}|$. The red and blue curves represent the first and third empirical quartiles of the absolute differences, respectively, and the yellow curve is the corresponding sample median curve. The differences can be seen to converge to zero for both estimators, but the moment estimator requires larger sample sizes for this. That is, the quartile Q_3 for the Hill estimator is close to zero already with $n = 10^5$ and, conversely, the moment estimator quartile Q_3 requires samples of size $n = 10^7$ for achieving the same magnitude.

6 Real data example

Heavy-tailed distributions are encountered frequently in the context of financial instruments (Rachev, 2003). Here, we consider extreme value index estimation for a four-dimensional financial time series downloaded from Yahoo Finance. The data consist of the daily log-returns of the S&P500 index and the stock prices of CISCO Systems, Intel Corporation and Sprint Corporation in the period of January 3rd, 1991 – September 12th, 2019. The observations were further standardized to have unit variance, which can be done without loss of generality as both our extreme value index estimators are scale invariant. A subset of the data from a shorter period of time was used already in Fan et al. (2008) in the context of multivariate volatility

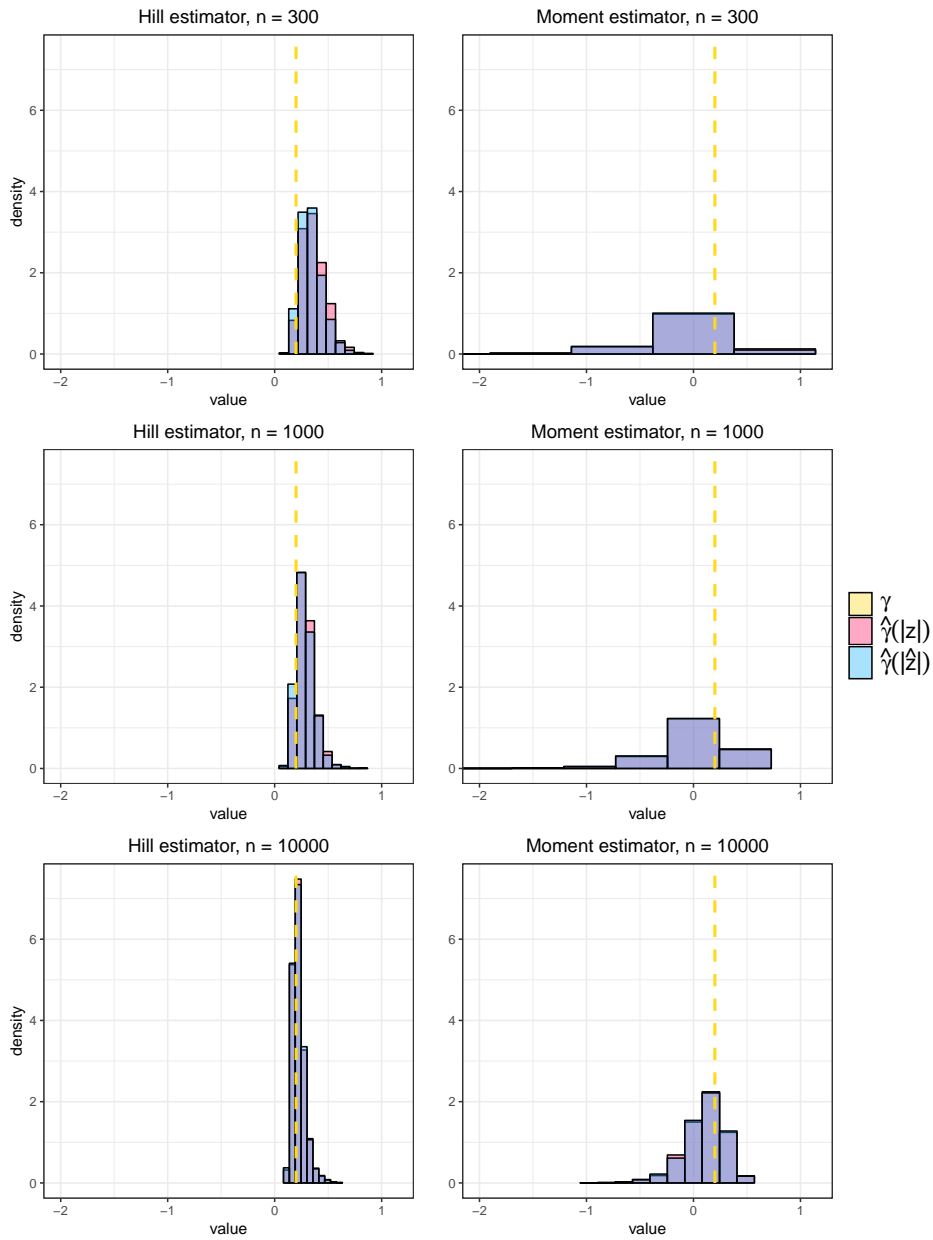


Figure 1: Histograms of $\hat{\gamma}(|\mathbf{z}|)$ (light red) and $\hat{\gamma}(|\hat{\mathbf{z}}|)$ (light blue) in the simulation study with sample sizes 300, 1000 and 10 000. The dashed yellow vertical line is the theoretical extreme value index $\gamma = 1/5$. The dark blue color in the histograms represents the area, where the two histograms overlap.

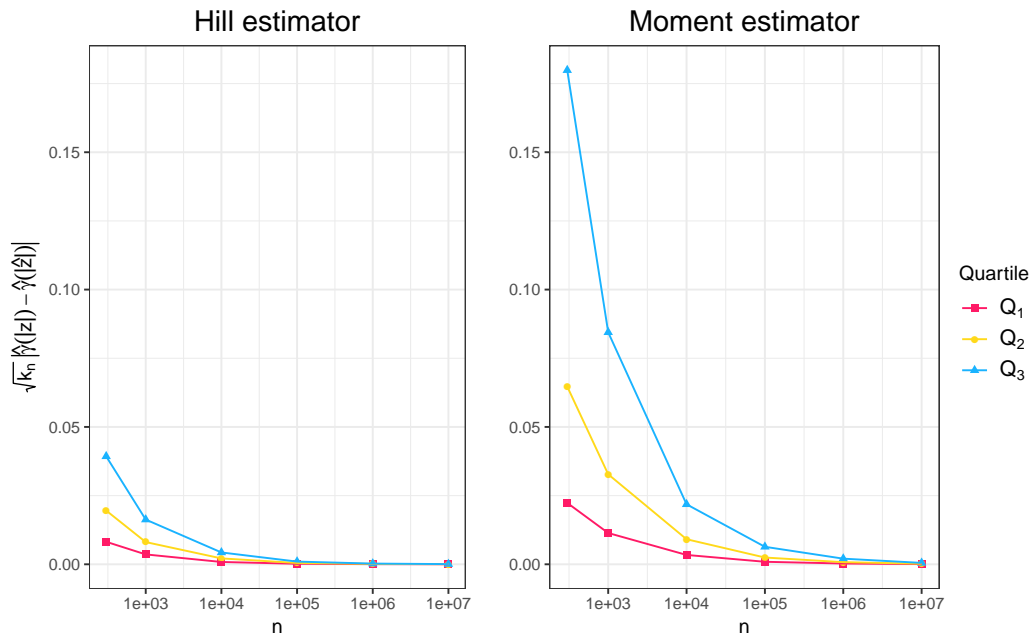


Figure 2: The quartiles of $\sqrt{k_n} |\hat{\gamma}(|\mathbf{z}|) - \hat{\gamma}(|\hat{\mathbf{z}}|)|$, for the Hill estimator and the moment estimator in the simulation study.

modeling, which inspired us to choose the same data set.

The full four-variate series is visualized in Figure C7 in the supplementary Appendix C. Volatility spikes that span most of the series occur around the years 2002 and 2008, caused by the stock market downturn of 2002 and the financial crisis of 2007–2008, respectively. Especially the latter time period stands out also in Figure 3, where we have estimated the extreme value indices of the individual series. The estimation in Figure 3 was conducted by moving a window of length 60 days through each univariate series and estimating the extreme value index of each window with the Hill estimator with the tail length $k_n = k = 16$. The x -axis values in the plot correspond to the middle days (30th days) of the windows. Contrary to the approach in Section 3, we estimated the extreme value indices not from the absolute values of the series, but separately for both the left and the right tail of each of the series. That is, for each of the four time series in Figure C7, we obtain two sequences of extreme value index estimates, always plotted with the same colours in Figure 3. This approach was taken to assess the behaviour of both negative and positive returns separately, in order to perform a more subtle analysis. Based on Figures 3 and C7, it seems reasonable to assume that among the four series there is an underlying latent factor (“financial crisis series”) which contributes risk to all four series around the times of the previous two crises.

To explore this, we estimate latent factors using generalized SOBI (Miettinen et al., 2019), an extension of the SOBI method which uses both serial correlation and volatility information in estimating the latent series. Denoting the original four-variate series at time i by \mathbf{x}_i , the estimates of the centered latent series are given by $\hat{\mathbf{z}}_i = \hat{\mathbf{\Gamma}}(\mathbf{x}_i - \bar{\mathbf{x}})$ where $\hat{\mathbf{\Gamma}} \in \mathbb{R}^{4 \times 4}$ is the unmixing matrix estimate given by generalized SOBI. The estimates are shown in Figure C8 in the supplementary Appendix C and indeed hint that the risk on certain periods is driven by individual latent factors. E.g., the majority of the volatility associated with the 2007-2008 financial crisis has concentrated in the fourth latent series.

To get a clearer view, Figure 4 shows the extreme value index estimates of the four latent series, obtained using the same rolling window approach as used in Figure 3. The most prominent feature in Figure 4 is the spike around year 2002 in one of the extreme value indices of the first series, indicating a period of large risk. Several other spikes are also visible, most notably in one of the indices of the fourth latent series during late 2002. Thus, we infer that the 2002 crisis was driven by two separate sources of risk.

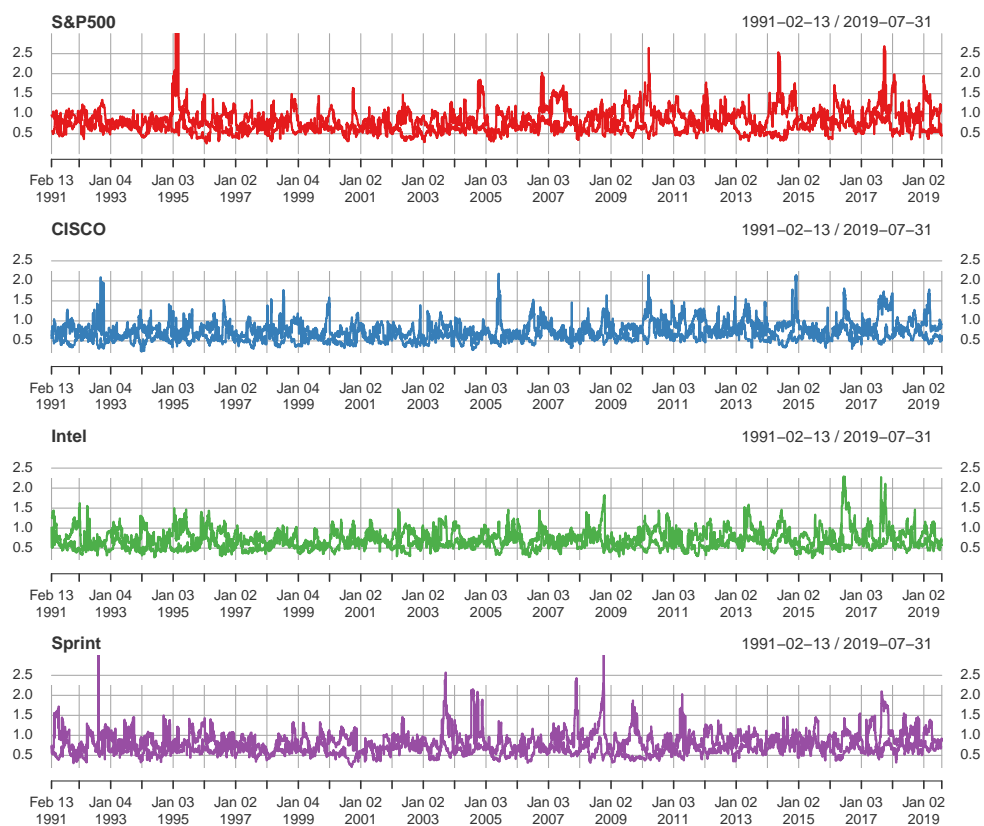


Figure 3: The extreme value indices of the observed series \mathbf{x}_i estimated with a rolling window of length 60 days. The two series in each plot correspond to the extreme value index estimates of the left and right tails of the corresponding series. Hill estimator with the tail length $k_n = 16$ was used. The x -axis in the plot denotes the middle (30th) days of the windows.



Figure 4: The extreme value indices of the latent series \mathbf{z}_i estimated with a rolling window of length 60 days. The two series in each plot correspond to the extreme value index estimates of the left and right tails of the corresponding series. Hill estimator with the tail length $k_n = 16$ was used. The x -axis in the plot denotes the middle (30th) days of the windows.

Finally, we study the connection between the factors and the observed series. The inverse transformation from the latent series to the observed ones is $\hat{\mathbf{x}}_i = \hat{\mathbf{\Gamma}}^{-1} \mathbf{z}_i + \bar{\mathbf{x}}$ where

$$\hat{\mathbf{\Gamma}}^{-1} = \begin{pmatrix} 0.54 & 0.16 & 0.20 & 0.80 \\ 0.24 & 0.87 & 0.28 & 0.34 \\ 0.28 & 0.16 & 0.89 & 0.32 \\ -0.51 & 0.04 & 0.10 & 0.85 \end{pmatrix},$$

contains the loadings of the latent sources for each of the observed series. The loadings reveal, for example, that both the first and fourth latent series contribute (absolutely) most to the first and the fourth original time series. More specifically, the fourth latent process is the most important (loadings 0.80 and 0.85), and the first latent process the second most important (loadings 0.54 and -0.51) in explaining the behavior of the log-returns of S&P500 and Sprint. We conclude that, out of the four observed series, the financial crises affected S&P500 and Sprint the most, and had a significantly smaller impact on CISCO and Intel.

7 Conclusion

We studied the effect of a preliminary latent variable extraction on the estimation of the extreme value indices of the latent independent components. This approach to multivariate extreme value analysis is highly practical in the sense that it reduces the problem into several univariate extreme value problems, allowing the use of the standard extreme value machinery. Moreover, our asymptotic analysis revealed that, under reasonably mild conditions, the consistency and limiting normality of the Hill estimator and the moment estimator are preserved in this construction.

A natural question to pursue in the future is whether the conditions in Theorems 2 and 3 can be weakened (we only showed that they are sufficient). Some preliminary simulation (not shown here) indicates that this might indeed be the case. Moreover, the current work can likely be used to simplify the task of deriving similar results for other suitable estimators besides the Hill estimator and the moment estimator. This is because the perturbation bounds for tail observations given in Appendix A.1 are not tied to any particular extreme value index estimator (indeed, they concern the latent variable

estimation part of the model). As such, one only needs to derive the analogues of Appendix A.2 (perturbation bounds for the actual extreme value index estimation step) for the new methods.

A Proofs

Section A of the appendix is devoted to the proofs of the technical results. We have gathered auxiliary technical lemmas into Subsection A.1 and Subsection A.2 contains to the proofs of our main theorems.

A.1 Auxiliary lemmas

The main objective in this subsection is to establish the rate at which the quantity

$$| |\hat{\mathbf{z}}^k|_{(n-m,n)} / |\mathbf{z}^k|_{(n-m,n)} - 1 |$$

vanishes. We begin with the next result that allows us to consider the component with the heaviest tail as the conservative bound for the error. This translates into $\max_l \{g_{nl}\}$ on our main theorems.

Lemma 1. *Let $F_0 \in G_{\gamma_0}, F_1 \in G_{\gamma_1}, F_2 \in G_{\gamma_2}, F_3 \in G_{\gamma_3}$ be distributions such that,*

$$\gamma_0 > \gamma_1 > \gamma_2 = 0 > \gamma_3.$$

For $k = 0, 1, 2, 3$, put $g_{nk} = \max\{a_{nk}, b_{nk}\}$, where a_{nk}, b_{nk} are the normalising sequences such that $\frac{y_{(n,n)}^k - b_{nk}}{a_{nk}} \rightsquigarrow G_{\gamma}$, where y^k follows F_k . Then

$$\frac{g_{nk}}{g_{n0}} = o(1), \quad k = 1, 2, 3.$$

Proof. Note first that since $\gamma_0 > 0$, the distribution F_0 is heavy tailed and belongs to the domain of attraction of the Fréchet distribution. Thus, by (Embrechts et al., 2013, Section 3.4), $g_{n0} = a_{n0} = n^{\gamma_0} L_0(n)$ where L_0 is a slowly varying function. Similarly $g_{n1} = n^{\gamma_1} L_1(n)$ for some slowly varying function L_1 and we have the claim for the value $k = 1$, that is,

$$\frac{g_{n1}}{g_{n0}} = n^{\gamma_1 - \gamma_0} \frac{L_1(n)}{L_0(n)} = o(1).$$

Similarly, the distribution F_3 is light tailed and belongs to the domain of attraction of the Weibull distribution. As such, by (Embrechts et al., 2013,

Section 3.4), we have $g_{n3} = \max\{n^{\gamma_3}L_3(n), d\}$ for some slowly-varying function L_3 and constant d . Since $\gamma_3 < 0$, we have $g_{n3} = \mathcal{O}(1)$ and the claim for $k = 3$ follows from

$$\frac{g_{n3}}{g_{n0}} = \frac{\mathcal{O}(1)}{n^{\gamma_0}L_0(n)} = o(1).$$

It remains to prove the case $k = 2$ that corresponds to the border case $\gamma_2 = 0$. Now F_2 belongs to the domain of attraction of the Gumbel distribution and, by (Embrechts et al., 2013, Section 3.4), we have $g_{n2} = \max\{a(b_n), b_n\}$, where $a(b_n)$ is as in (Embrechts et al., 2013, Definition 3.3.18), $b_n = F_2^{\leftarrow}(1 - 1/n)$ and F_2^{\leftarrow} is the quantile function. Let $y_F \leq \infty$ be the right endpoint of the distribution F_2 . We consider two cases, $y_F < \infty$ and $y_F = \infty$, separately. In the former, $b_n \rightarrow y_F$ as $n \rightarrow \infty$ and by (Embrechts et al., 2013, Remark 2, Section 3.3) $a(b_n) \rightarrow 0$ as $n \rightarrow \infty$. Thus, for a large enough n , we have $g_{n2} = b_n \rightarrow y_F < \infty$ and

$$\frac{g_{n2}}{g_{n0}} = \frac{y_F + o(1)}{n^{\gamma_0}L_0(n)} = o(1).$$

For $y_F = \infty$, we have $b_n \rightarrow \infty$ and, by (Embrechts et al., 2013, Remark 1, Section 3.3), $a(b_n) = o(b_n)$. Thus, for a large enough n , we have $g_{n2} = b_n$ and

$$\frac{g_{n2}}{g_{n0}} = \frac{F_2^{\leftarrow}(1 - 1/n)}{n^{\gamma_0}L_0(n)}.$$

We continue by proof by contradiction, and assume that $\frac{F_2^{\leftarrow}(1-1/n)}{n^{\gamma_0}L_0(n)}$ does not converge to zero. Then there exists $\epsilon_0 > 0$ such that we can find an arbitrarily large n such that

$$F_2^{\leftarrow}(1 - 1/n) \geq \epsilon_0 n^{\gamma_0} L_0(n).$$

It follows that

$$1 - F_2(\epsilon_0 n^{\gamma_0} L_0(n)) \geq \frac{1}{n}$$

and since L_0 is slowly varying, this further implies that

$$1 - F_2(cn^{\gamma_0}) \geq \frac{1}{n}$$

for some constant $c > 0$ and a large enough n . Since $\gamma_0 > 0$, this implies that F_2 is heavy tailed giving us the contradiction. This completes the proof for the case $k = 2$ as well. \square

The next result shows that the denominator in $|\hat{\mathbf{z}}^k|_{(n-m,n)}/|\mathbf{z}^k|_{(n-m,n)} - 1$ is negligible.

Lemma 2. *Let $(z_k), k = 1, \dots, n$ be an arbitrary sequence of non-negative random variables such that*

$$\liminf_{\delta \rightarrow 0} \mathbb{P}(z_k \geq \delta) = 1. \quad (14)$$

Then, for any $\epsilon > 0$ and any intermediate sequence k_n , there exists $\delta > 0$ and N such that

$$\mathbb{P}(z_{(n-k_n,n)} < \delta) < \epsilon, \quad n \geq N.$$

Proof. Let

$$S_n(\delta) = \sum_{k=1}^n \mathbf{1}_{z_k \geq \delta}.$$

Then

$$\mathbb{P}(z_{(n-k_n,n)} < \delta) = \mathbb{P}(S_n(\delta) < k_n).$$

Indeed, $S_n(\delta) < k_n$ means that less than k_n of the values are above or equal to δ , which implies that k_n :th maximum of z is strictly less than δ . Vice versa, if $z_{(n-k_n,n)} < \delta$, then at most $k_n - 1$ of values z_k can be above or equal to δ . Thus it suffices to prove that for any $\epsilon > 0$, we can find N and δ such that for $n \geq N$ we have

$$\mathbb{P}(S_n(\delta) < k_n) < \epsilon.$$

Equivalently, we need to show

$$\mathbb{P}(S_n(\delta) \geq k_n) > 1 - \epsilon. \quad (15)$$

Denote $\bar{S}_n(\delta) = \frac{S_n(\delta)}{n}$. By (14), for any $\tilde{\epsilon} > 0$ we can find $\delta > 0$ small enough such that

$$\mathbb{E}\bar{S}_n(\delta) = \frac{1}{n} \sum_{k=1}^n \mathbb{P}(z_k \geq \delta) > 1 - \tilde{\epsilon} \quad (16)$$

uniformly in n . Together with $\bar{S}_n(\delta) \leq 1$ this gives us

$$\frac{[\mathbb{E}\bar{S}_n(\delta)]^2}{\mathbb{E}\bar{S}_n^2(\delta)} \geq (1 - \tilde{\epsilon})^2$$

which holds for every n . Next we recall the Paley-Zygmund inequality which states that, for any random variable $Z \geq 0$ with finite variance and any number $\theta \in [0, 1]$, we have

$$\mathbb{P}(Z \geq \theta \mathbb{E}Z) \geq (1 - \theta)^2 \frac{(\mathbb{E}Z)^2}{\mathbb{E}Z^2}. \quad (17)$$

Since k_n is an intermediate sequence, we have, applying (16), that

$$\frac{k_n}{n\mathbb{E}\bar{S}_n(\delta)} \leq \frac{k_n}{n(1 - \tilde{\epsilon})} \leq 1$$

provided that n is large enough. Hence we may apply (17) with $Z = \bar{S}_n(\delta)$ and $\theta = \frac{k_n}{n\mathbb{E}\bar{S}_n(\delta)}$ to compute

$$\begin{aligned} \mathbb{P}(S_n(\delta) \geq k_n) &= \mathbb{P}\left(\bar{S}_n(\delta) \geq \frac{k_n}{n\mathbb{E}\bar{S}_n(\delta)} \mathbb{E}\bar{S}_n(\delta)\right) \\ &\geq \left(1 - \frac{k_n}{n\mathbb{E}\bar{S}_n(\delta)}\right)^2 \frac{[\mathbb{E}\bar{S}_n(\delta)]^2}{\mathbb{E}\bar{S}_n^2(\delta)} \\ &\geq \left(1 - \frac{k_n}{n(1 - \tilde{\epsilon})}\right)^2 (1 - \tilde{\epsilon})^2. \end{aligned}$$

This implies (15), since $\tilde{\epsilon} > 0$ can be chosen arbitrarily and independently of n . This concludes the proof. \square

The next two results allow us to deduce bounds for the difference between order statistics of $|\hat{\mathbf{z}}^k|$ and $|\mathbf{z}^k|$.

Lemma 3. *Let $\mathbf{a} = (a_1, \dots, a_n)$ and $\mathbf{b} = (b_1, \dots, b_n)$ satisfy $a_i \leq b_i$, for all $i = 1, \dots, n$. Then*

$$(\mathbf{a})_{(k,n)} \leq (\mathbf{b})_{(k,n)},$$

for all $k = 1, \dots, n$.

Proof. Recall Weyl's inequality: if $\mathbf{R}, \mathbf{S} \in \mathbb{R}^{n \times n}$ are symmetric matrices and $\lambda_j(\mathbf{R})$ denotes the j th largest eigenvalue of the matrix \mathbf{R} , $j = 1, \dots, n$, then

$$\lambda_{j+m}(\mathbf{R}) + \lambda_{k-m}(\mathbf{S}) \leq \lambda_j(\mathbf{R} + \mathbf{S}) \leq \lambda_{j-\ell}(\mathbf{R}) + \lambda_{1+\ell}(\mathbf{S}).$$

for all $\ell = 0, \dots, j - 1, m = 0, \dots, k - j$, see Horn and Johnson (1990).

Let $\text{diag}(\mathbf{r}) \in \mathbb{R}^{n \times n}$ denote the diagonal matrix having the elements of the vector $\mathbf{r} = (r_1, \dots, r_n)$ as its diagonal elements. Then $(\mathbf{r})_{(k,n)} = \lambda_{n-k+1}[\text{diag}(\mathbf{r})]$ and the right-hand side of Weyl's inequality with $j = n-k+1$ and $\ell = 0$ gives,

$$(\mathbf{r} + \mathbf{s})_{(k,n)} \leq (\mathbf{r})_{(k,n)} + (\mathbf{s})_{(n,n)}, \quad (18)$$

for any two vectors $\mathbf{r} = (r_1, \dots, r_n)$ and $\mathbf{s} = (s_1, \dots, s_n)$.

Apply next (18) to $\mathbf{r} = \mathbf{b}$ and $\mathbf{s} = \mathbf{a} - \mathbf{b}$ to obtain the claim,

$$(\mathbf{a})_{(k,n)} \leq (\mathbf{b})_{(k,n)} + (\mathbf{a} - \mathbf{b})_{(n,n)} \leq (\mathbf{b})_{(k,n)},$$

where the second inequality holds as all elements of the sequence $\mathbf{a} - \mathbf{b}$ are non-positive. \square

Lemma 4. *Let $\mathbf{x} = (x_1, \dots, x_n)$ and $\boldsymbol{\epsilon} = (\epsilon_1, \dots, \epsilon_n)$ be arbitrary. Then for all $k = 1, \dots, n$,*

$$\left| |\mathbf{x} + \boldsymbol{\epsilon}|_{(k,n)} - |\mathbf{x}|_{(k,n)} \right| \leq |\boldsymbol{\epsilon}|_{(n,n)},$$

where for a vector $\mathbf{a} = (a_1, \dots, a_n)$ the notation $|\mathbf{a}| \in \mathbb{R}^n$ refers to the vector of the element-wise absolute values of \mathbf{a} .

Proof. Equation (18) with $\mathbf{r} = |\mathbf{x}|$ and $\mathbf{s} = |\boldsymbol{\epsilon}|$ in conjunction with the triangle inequality, $|x_i + \epsilon_i| \leq |x_i| + |\epsilon_i|$, and Lemma 3 allow us to estimate,

$$|\mathbf{x} + \boldsymbol{\epsilon}|_{(k,n)} - |\mathbf{x}|_{(k,n)} \leq (|\mathbf{x}| + |\boldsymbol{\epsilon}|)_{(k,n)} - |\mathbf{x}|_{(k,n)} \leq |\boldsymbol{\epsilon}|_{(n,n)},$$

giving the first half of the inequality. For the other half, we have by the same set of inequalities and the expansion $\mathbf{x} = \mathbf{x} + \boldsymbol{\epsilon} - \boldsymbol{\epsilon}$,

$$|\mathbf{x}|_{(k,n)} - |\mathbf{x} + \boldsymbol{\epsilon}|_{(k,n)} \leq (|\mathbf{x} + \boldsymbol{\epsilon}| + |\boldsymbol{\epsilon}|)_{(k,n)} - |\mathbf{x} + \boldsymbol{\epsilon}|_{(k,n)} \leq |\boldsymbol{\epsilon}|_{(n,n)},$$

where the second inequality is obtained by applying (18) to $\mathbf{r} = |\mathbf{x} + \boldsymbol{\epsilon}|$ and $\mathbf{s} = |\boldsymbol{\epsilon}|$. \square

Combining previous results yields the following lemma that provides a crucial estimate for the proofs of our main theorems.

Lemma 5. *Let $k = 1, \dots, p$ be fixed. Then, under (3) and Assumption 1, we have*

$$\max_{0 \leq m \leq k_n} \left| \frac{|\hat{\mathbf{z}}^k|_{(n-m,n)}}{|\mathbf{z}^k|_{(n-m,n)}} - 1 \right| = \mathcal{O}_p \left(\frac{1}{c_n} \max_{\ell} \{g_{n\ell}\} \right).$$

Proof. The left-hand side of the claim equals

$$\max_{0 \leq m \leq k_n} \left| \frac{|\hat{\mathbf{z}}^k|_{(n-m,n)} - |\mathbf{z}^k|_{(n-m,n)}}{|\mathbf{z}^k|_{(n-m,n)}} \right|, \quad (19)$$

where by (3) and Lemma 4 the numerator can be bounded by

$$\left| |\hat{\mathbf{z}}^k|_{(n-m,n)} - |\mathbf{z}^k|_{(n-m,n)} \right| \leq \max_i \left\{ \left| \sum_{j=1}^p \hat{h}_j z_{ij} + \hat{r} \right| \right\} \leq \sum_{j=1}^p |\hat{h}_j| |\mathbf{z}^j|_{(n,n)} + |\hat{r}|,$$

where $\hat{h}_j = \mathcal{O}_p(c_n^{-1})$, $j = 1, \dots, p$, and $\hat{r} = \mathcal{O}_p(c_n^{-1})$. Now, by Assumption 1, we have

$$\begin{aligned} & \sum_{j=1}^p |\hat{h}_j| |\mathbf{z}^j|_{(n,n)} + |\hat{r}| \\ &= \sum_{j=1}^p \left(a_{nj} |\hat{h}_j| \frac{|\mathbf{z}^j|_{(n,n)} - b_{nj}}{a_{nj}} + |\hat{h}_j| b_{nj} \right) + |\hat{r}| \\ &= \sum_{j=1}^p \left(\frac{a_{nj}}{c_n} \mathcal{O}_p(1) + \frac{b_{nj}}{c_n} \mathcal{O}_p(1) \right) + \mathcal{O}_p\left(\frac{1}{c_n}\right) \\ &= \sum_{j=1}^p \mathcal{O}_p\left(\frac{g_{nj}}{c_n}\right) + \mathcal{O}_p\left(\frac{1}{c_n}\right) \\ &= \mathcal{O}_p\left(\frac{1}{c_n} \max_{\ell} \{g_{n\ell}\}\right), \end{aligned}$$

where we have used the result that if one deterministic sequence eventually majorizes another, $r_n \leq s_n$, for all $n \geq N$, then any sequence of random variables x_n with $x_n = \mathcal{O}_p(r_n)$ has also $x_n = \mathcal{O}_p(s_n)$.

The previous bound holds uniformly in m . Thus

$$\max_{0 \leq m \leq k_n} \left| \frac{|\hat{\mathbf{z}}^k|_{(n-m,n)} - |\mathbf{z}^k|_{(n-m,n)}}{|\mathbf{z}^k|_{(n-m,n)}} \right| = \mathcal{O}_p\left(\frac{1}{c_n} \max_{\ell} \{g_{n\ell}\}\right) \max_{0 \leq m \leq k_n} \frac{1}{|\mathbf{z}^1|_{(n-m,n)}},$$

where $\max_{0 \leq m \leq k_n} |\mathbf{z}^1|_{(n-m,n)}^{-1} = |\mathbf{z}^1|_{(n-k_n,n)}^{-1}$ is, by Lemma 2, of order $\mathcal{O}_p(1)$. This concludes the proof. \square

Finally, we end this section with the following result allowing us to handle logarithm in the estimators.

Lemma 6. *Let x_n be an arbitrary triangular array of random variables satisfying $\max_{0 \leq m \leq d_n} |x_m| = \mathcal{O}_p(e_n)$ for some d_n and $e_n = o(1)$. Furthermore, let $g : (a, b) \mapsto \mathbb{R}$ with $-\infty \leq a < 0 < b \leq \infty$ be such that g is continuously differentiable at the neighbourhood of 0. Then*

$$\max_{0 \leq m \leq d_n} |g(x_m) - g(0)| = \mathcal{O}_p(e_n).$$

Proof. Let $\epsilon > 0$ be fixed. Then there exists $C > 0$ and N such that

$$\mathbb{P} \left(\frac{\max_{0 \leq m \leq d_n} |x_m|}{e_n} > C \right) < \frac{\epsilon}{2}$$

for $n \geq N$. By assumptions, there exists $\delta > 0$ such that g is continuously differentiable on an open interval $(-\delta, \delta)$. Moreover, by continuity of g' we also have

$$(g')^* = \sup_{-\frac{\delta}{2} \leq x \leq \frac{\delta}{2}} |g'(x)| < \infty.$$

Moreover, since $e_n = o(1)$ there exists N^* such that $e_n C \leq \frac{\delta}{2}$ for $n \geq N^*$. Thus, on the set $A_n = \{\max_{0 \leq m \leq d_n} |x_m| \leq e_n C\}$ mean value theorem implies

$$\max_{0 \leq m \leq d_n} |g(x_m) - g(0)| \leq (g')^* \max_{0 \leq m \leq d_n} |x_m|.$$

Let $n \geq \max(N, N^*)$ and put $\tilde{C} = (g')^* C$. We have

$$\begin{aligned} & \mathbb{P} \left(\frac{\max_{0 \leq m \leq d_n} |g(x_m) - g(0)|}{e_n} > \tilde{C} \right) \\ &= \mathbb{P} \left(A_n, \frac{\max_{0 \leq m \leq d_n} |g(x_m) - g(0)|}{e_n} > \tilde{C} \right) + \mathbb{P} \left(A_n^c, \frac{\max_{0 \leq m \leq d_n} |g(x_m) - g(0)|}{e_n} > \tilde{C} \right) \\ &\leq \mathbb{P} \left(A_n, \frac{(g')^* \max_{0 \leq m \leq d_n} |x_m|}{e_n} > \tilde{C} \right) + \mathbb{P}(A_n^c) \\ &\leq \mathbb{P} \left(\frac{\max_{0 \leq m \leq d_n} |x_m|}{e_n} > C \right) + \mathbb{P} \left(\frac{\max_{0 \leq m \leq d_n} |x_m|}{e_n} > C \right) \\ &< \epsilon \end{aligned}$$

concluding the proof. \square

A.2 Convergence of the Hill and Moment estimators

We begin with the proof of Theorem 2.

Proof of Theorem 2. Let $\mathbf{y} = (y_1, \dots, y_n) \geq 0$ and $\hat{\mathbf{y}} = (\hat{y}_1, \dots, \hat{y}_n) \geq 0$ be an arbitrary pair of samples that satisfy

$$\max_{0 \leq m \leq k_n} \left| \frac{(\hat{\mathbf{y}})_{(n-m,n)}}{(\mathbf{y})_{(n-m,n)}} - 1 \right| = \mathcal{O}_p(h_n), \quad (20)$$

where $h_n = o(1)$.

Recall that the Hill estimator is given by

$$\hat{\gamma}_H(\mathbf{y}) = M_n^{(1)}(\mathbf{y}) = \frac{1}{k_n} \sum_{m=0}^{k_n-1} \log \frac{(\mathbf{y})_{(n-m,n)}}{(\mathbf{y})_{(n-k_n,n)}},$$

where $k_n/n \rightarrow 0$, $k_n \rightarrow \infty$. In the proof, we use the short notation

$$\hat{w}_m := \frac{(\hat{\mathbf{y}})_{(n-m,n)}}{(\mathbf{y})_{(n-m,n)}} - 1.$$

We now have

$$\begin{aligned} |M_n^{(1)}(\hat{\mathbf{y}}) - M_n^{(1)}(\mathbf{y})| &= \left| \frac{1}{k_n} \sum_{m=0}^{k_n-1} \left[\log \frac{(\hat{\mathbf{y}})_{(n-m,n)}}{(\hat{\mathbf{y}})_{(n-k_n,n)}} - \log \frac{(\mathbf{y})_{(n-m,n)}}{(\mathbf{y})_{(n-k_n,n)}} \right] \right| \\ &= \left| \frac{1}{k_n} \sum_{m=0}^{k_n-1} [\log(1 + \hat{w}_m) - \log(1 + \hat{w}_{k_n})] \right| \\ &\leq \frac{1}{k_n} \sum_{m=0}^{k_n-1} (|\log(1 + \hat{w}_m)| + |\log(1 + \hat{w}_{k_n})|) \\ &\leq 2 \max_{0 \leq m \leq k_n} |\log(1 + \hat{w}_m)|. \end{aligned}$$

The assumptions of Lemma 6 are now satisfied for $x_n = \hat{w}_n$, $d_n = k_n$, $e_n = h_n$ and $g(x) = \log(1+x)$, implying that $|M_n^{(1)}(\hat{\mathbf{y}}) - M_n^{(1)}(\mathbf{y})| = \mathcal{O}_p(h_n)$. Plugging in $\mathbf{y} = \mathbf{z}^k$ and $\hat{\mathbf{y}} = \hat{\mathbf{z}}^k$, and using Lemma 5, now give the convergence of the Hill estimator. For the moment estimator, recall that

$$\hat{\gamma}_M(\mathbf{y}) = M_n^{(1)}(\mathbf{y}) + 1 - \frac{1}{2} \left(1 - \frac{[M_n^{(1)}(\mathbf{y})]^2}{M_n^{(2)}(\mathbf{y})} \right)^{-1}.$$

By the first part of the proof, we have

$$|M_n^{(1)}(\hat{\mathbf{y}}) - M_n^{(1)}(\mathbf{y})| = \mathcal{O}_p(h_n). \quad (21)$$

It thus suffices to prove that

$$\left| \frac{[M_n^{(1)}(\mathbf{y})]^2}{M_n^{(2)}(\mathbf{y})} - \frac{[M_n^{(1)}(\hat{\mathbf{y}})]^2}{M_n^{(2)}(\hat{\mathbf{y}})} \right| = \mathcal{O}_p\left(\frac{h_n}{\hat{\gamma}_H(\mathbf{y})}\right). \quad (22)$$

Indeed, since $M_n^{(1)}(\mathbf{y}) = \hat{\gamma}_H(\mathbf{y})$ as a convergent sequence is uniformly tight, i.e., $\mathcal{O}_p(1)$, it follows from the convergence of $\hat{\gamma}_M(\mathbf{y})$ that

$$\left(1 - \frac{[M_n^{(1)}(\mathbf{y})]^2}{M_n^{(2)}(\mathbf{y})}\right)^{-1} = \mathcal{O}_p(1).$$

Then (22) together with the assumption $\frac{h_n}{\hat{\gamma}_H(\mathbf{y})} \rightarrow_p 0$ implies that also

$$\left(1 - \frac{[M_n^{(1)}(\hat{\mathbf{y}})]^2}{M_n^{(2)}(\hat{\mathbf{y}})}\right)^{-1} = \mathcal{O}_p(1).$$

The claim then follows by using

$$(1 - a)^{-1} - (1 - b)^{-1} = \frac{a - b}{1 - a}(1 - b)^{-1}, \quad a, b \in (0, 1)$$

with $a = \frac{[M_n^{(1)}(\mathbf{y})]^2}{M_n^{(2)}(\mathbf{y})}$ and $b = \frac{[M_n^{(1)}(\hat{\mathbf{y}})]^2}{M_n^{(2)}(\hat{\mathbf{y}})}$, leading to

$$|\hat{\gamma}_M(\hat{\mathbf{y}}) - \hat{\gamma}_M(\mathbf{y})| = \mathcal{O}_p\left(\frac{h_n}{\hat{\gamma}_H(\mathbf{y})}\right). \quad (23)$$

In order to prove (22) we write

$$\begin{aligned} \left| \frac{[M_n^{(1)}(\mathbf{y})]^2}{M_n^{(2)}(\mathbf{y})} - \frac{[M_n^{(1)}(\hat{\mathbf{y}})]^2}{M_n^{(2)}(\hat{\mathbf{y}})} \right| &\leq \frac{1}{M_n^{(2)}(\mathbf{y})} \left| [M_n^{(1)}(\mathbf{y})]^2 - [M_n^{(1)}(\hat{\mathbf{y}})]^2 \right| \\ &\quad + \frac{[M_n^{(1)}(\hat{\mathbf{y}})]^2}{M_n^{(2)}(\hat{\mathbf{y}})M_n^{(2)}(\mathbf{y})} \left| M_n^{(2)}(\mathbf{y}) - M_n^{(2)}(\hat{\mathbf{y}}) \right| \\ &=: I_1(n) + I_2(n). \end{aligned}$$

For the first term $I_1(n)$, we use $a^2 - b^2 = (a - b)(a + b)$ and (21) to get

$$\begin{aligned} | [M_n^{(1)}(\mathbf{y})]^2 - M_n^{(1)}(\hat{\mathbf{y}})]^2 | &= | M_n^{(1)}(\mathbf{y}) - M_n^{(1)}(\hat{\mathbf{y}}) | | M_n^{(1)}(\mathbf{y}) + M_n^{(1)}(\hat{\mathbf{y}}) | \\ &\leq | M_n^{(1)}(\mathbf{y}) - M_n^{(1)}(\hat{\mathbf{y}}) |^2 + 2 | M_n^{(1)}(\mathbf{y}) - M_n^{(1)}(\hat{\mathbf{y}}) | M_n^{(1)}(\mathbf{y}) \\ &= \mathcal{O}_p \left(h_n M_n^{(1)}(\mathbf{y}) \right). \end{aligned}$$

Here we used also the fact that $\frac{h_n}{M_n^{(1)}(\mathbf{y})} \rightarrow_p 0$. Moreover, by Cauchy-Schwarz inequality we have $[M_n^{(1)}(\mathbf{y})]^2 \leq M_n^{(2)}(\mathbf{y})$. Thus we can estimate

$$\begin{aligned} I_1(n) &= \frac{1}{M_n^{(2)}(\mathbf{y})} | [M_n^{(1)}(\mathbf{y})]^2 - M_n^{(1)}(\hat{\mathbf{y}})]^2 | \\ &\leq \frac{1}{[M_n^{(1)}(\mathbf{y})]^2} \mathcal{O}_p \left(h_n M_n^{(1)}(\mathbf{y}) \right) \\ &= \mathcal{O}_p \left(\frac{h_n}{M_n^{(1)}(\mathbf{y})} \right) \end{aligned}$$

which, by recalling that $\hat{\gamma}_H(\mathbf{y}) = M_n^{(1)}(\mathbf{y})$, gives the claim for the term $I_1(n)$. For the term $I_2(n)$, we apply $a^2 - b^2 = (a - b)(a + b)$ again yielding

$$\begin{aligned} &| M_n^{(2)}(\hat{\mathbf{y}}) - M_n^{(2)}(\mathbf{y}) | \\ &= \left| \frac{1}{k_n} \sum_{m=0}^{k_n-1} \left[\left[\log \frac{(\hat{\mathbf{y}})_{(n-m,n)}}{(\hat{\mathbf{y}})_{(n-k_n,n)}} \right]^2 - \left[\log \frac{(\mathbf{y})_{(n-m,n)}}{(\mathbf{y})_{(n-k_n,n)}} \right]^2 \right] \right| \\ &\leq \frac{1}{k_n} \sum_{m=0}^{k_n-1} | \log(1 + \hat{w}_m) - \log(1 + \hat{w}_{k_n}) | \left| \log \frac{(\hat{\mathbf{y}})_{(n-m,n)}}{(\hat{\mathbf{y}})_{(n-k_n,n)}} + \log \frac{(\mathbf{y})_{(n-m,n)}}{(\mathbf{y})_{(n-k_n,n)}} \right| \\ &\leq \frac{2 \max_{0 \leq m \leq k_n} | \log(1 + \hat{w}_m) |}{k_n} \sum_{m=0}^{k_n-1} \left| \log \frac{(\hat{\mathbf{y}})_{(n-m,n)}}{(\hat{\mathbf{y}})_{(n-k_n,n)}} + \log \frac{(\mathbf{y})_{(n-m,n)}}{(\mathbf{y})_{(n-k_n,n)}} \right|. \end{aligned}$$

Here

$$\begin{aligned}
& \frac{1}{k_n} \sum_{m=0}^{k_n-1} \left| \log \frac{(\hat{\mathbf{y}})_{(n-m,n)}}{(\hat{\mathbf{y}})_{(n-k_n,n)}} + \log \frac{(\mathbf{y})_{(n-m,n)}}{(\mathbf{y})_{(n-k_n,n)}} \right| \\
& \leq \frac{1}{k_n} \sum_{m=0}^{k_n-1} \left| \log \frac{(\hat{\mathbf{y}})_{(n-m,n)}}{(\hat{\mathbf{y}})_{(n-k_n,n)}} - \log \frac{(\mathbf{y})_{(n-m,n)}}{(\mathbf{y})_{(n-k_n,n)}} \right| \\
& \quad + \frac{2}{k_n} \sum_{m=0}^{k_n-1} \log \frac{(\mathbf{y})_{(n-m,n)}}{(\mathbf{y})_{(n-k_n,n)}} \\
& \leq 2 \max_{0 \leq m \leq k_n} |\log(1 + \hat{u}_m)| + 2M_n^{(1)}(\mathbf{y}).
\end{aligned}$$

Together with Lemma 6 this gives us

$$|M_n^{(2)}(\hat{\mathbf{y}}) - M_n^{(2)}(\mathbf{y})| \leq \mathcal{O}_p(h_n M_n^{(1)}(\mathbf{y})).$$

Applying Cauchy-Schwarz again to get $[M_n^{(1)}(\hat{\mathbf{y}})]^2 \leq M_n^{(2)}(\hat{\mathbf{y}})$ gives us

$$\begin{aligned}
I_2(n) &= \frac{[M_n^{(1)}(\hat{\mathbf{y}})]^2}{M_n^{(2)}(\hat{\mathbf{y}})M_n^{(2)}(\mathbf{y})} |M_n^{(2)}(\mathbf{y}) - M_n^{(2)}(\hat{\mathbf{y}})| \\
&\leq \frac{1}{[M_n^{(1)}(\mathbf{y})]^2} |M_n^{(2)}(\mathbf{y}) - M_n^{(2)}(\hat{\mathbf{y}})| \\
&= \mathcal{O}_p\left(\frac{h_n}{M_n^{(1)}(\mathbf{y})}\right).
\end{aligned}$$

Plugging in $\mathbf{y} = \mathbf{z}^k$ and $\hat{\mathbf{y}} = \hat{\mathbf{z}}^k$, and using Lemma 5, now give the convergence of the moment estimator. This completes the proof. \square

Applying the above computations, the proof of Theorem 3 is now rather simple.

Proof of Theorem 3. We write

$$\sqrt{k_n} (\hat{\gamma}_H(|\hat{\mathbf{z}}^1|) - C_H) = \sqrt{k_n} (\hat{\gamma}_H(|\hat{\mathbf{z}}^1|) - \hat{\gamma}_H(|\mathbf{z}^1|)) + \sqrt{k_n} (\hat{\gamma}_H(|\mathbf{z}^1|) - C_H).$$

The first claim now follows directly from (21). Similarly, the second claim follows directly from

$$\sqrt{k_n} (\hat{\gamma}_M(|\hat{\mathbf{z}}^1|) - C_M) = \sqrt{k_n} (\hat{\gamma}_M(|\hat{\mathbf{z}}^1|) - \hat{\gamma}_M(|\mathbf{z}^1|)) + \sqrt{k_n} (\hat{\gamma}_M(|\mathbf{z}^1|) - C_M)$$

together with (23). \square

B Auxiliary simulation

The auxiliary simulation is otherwise similar to the simulation study in the main text, but is conducted with i.i.d. vectors instead of time-dependent series, putting us in the context of Section 4.1

Let $\tilde{\mathbf{z}}_1, \dots, \tilde{\mathbf{z}}_n$ be a collection of i.i.d. random vectors whose marginal distributions are independent and distributed as

$$\tilde{\mathbf{z}}_j = \left(\text{Pareto}(5) \quad \text{Pareto}(15) \quad \text{Pareto}(30) \right)^\top,$$

where $\text{Pareto}(\alpha)$ denotes the Pareto distribution with shape parameter α , scale parameter 1 and location parameter 0. Hereby, in this simulation setting, the first component has the heaviest tail and the corresponding theoretical extreme value index is $1/5$.

The simulation was conducted with six distinct sample sizes n , which were $300, 10^3, 10^4, 10^5, 10^6$ and 10^7 . The threshold sequence k_n was again chosen to be $k_n = \lfloor n^{1/4} \rfloor$ and, for each sample size, the simulation was iterated 2000 times.

As a preliminary step, the simulated observations $\tilde{\mathbf{z}}_j$ were centered. Here, the centered observations are denoted as \mathbf{z}_i . In every iteration $h \in \{1, \dots, 2000\}$, we applied the following linear transformation,

$$\mathbf{x}_i = \mathbf{\Omega}_h \mathbf{z}_i, \quad \forall i \in \{1, \dots, n\},$$

where the elements of the $\mathbb{R}^{3 \times 3}$ -matrix $\mathbf{\Omega}$ were simulated independently, and separately in every iteration, from the univariate uniform distribution $\text{unif}(-100, 100)$.

We then applied the FastICA procedure, implemented in the R package `fICA` (Miettinen et al., 2017), to the mixed observations $\mathbf{x}_1, \dots, \mathbf{x}_n$. Note that the asymptotic convergence of FastICA requires that all of the components have finite fourth moments. In this simulation study, the existence of the required moments is satisfied, as even the most heavy tailed component $\text{Pareto}(5)$ has finite fourth moments.

For a small number of iterations, the FastICA algorithm failed to converge. In the case of a failed FastICA convergence, the observations and the mixing matrix were simulated again, until 2000 successful FastICA estimates were obtained. We denote the observations unmixed by FastICA as $\hat{\mathbf{z}}_1, \dots, \hat{\mathbf{z}}_n$. In the sequel, we use the notations $|\hat{\mathbf{z}}|$ and $|\mathbf{z}|$ for the sets

$\{|\hat{\mathbf{z}}_1|, \dots, |\hat{\mathbf{z}}_n|\}$ and $\{|\mathbf{z}_1|, \dots, |\mathbf{z}_n|\}$, respectively. Here, the absolute value of a vector is taken elementwise.

In this simulation study, we have $\max_\ell(g_{n\ell}) = n^{-1/5}$, which corresponds to the `Pareto(5)` distribution. Furthermore, the FastICA unmixing estimator is \sqrt{n} -consistent, which gives $c_n = \sqrt{n}$. Hereby, under our choice of $k_n = \lfloor n^{1/4} \rfloor$, the assumptions required by Theorems 2 and 3 hold. Thus, under large sample sizes, the independent component estimation should have a negligible effect on the extreme value index estimation. This implies that, for large sample sizes, the extreme value index estimates calculated from $|\hat{\mathbf{z}}|$ and $|\mathbf{z}|$ are expected to be close to each other.

We estimated the extreme value indices for every component from both $|\hat{\mathbf{z}}|$ and $|\mathbf{z}|$, using both the Hill estimator and the moment estimator. Note that, both the Hill and the moment estimator produce three extreme value index estimates, one for each component. Thus, in every simulation iteration, we again collected the largest of the three extreme value index estimates, denoted in the following by $\hat{\gamma}(|\hat{\mathbf{z}}|)$ and $\hat{\gamma}(|\mathbf{z}|)$. Their histograms for sample sizes $n = 300, 10^3, 10^4$ are displayed in Figure B5.

In Figure B5, the extreme value indices estimated from $|\hat{\mathbf{z}}|$ are illustrated using light blue colour, and the extreme value index estimates calculated from the original $|\mathbf{z}|$ are illustrated using light red colour. Furthermore, the dark blue colour illustrates the proportion of estimates that overlap and the dashed yellow vertical line represents the theoretical extreme value index value $\gamma = 1/5$. Values smaller than -2 are omitted from the figure, as only a total of 5 moment estimates were smaller than -2 .

In Figure B5, already with sample size $n = 300$, the two histograms overlap almost completely. Moreover, when sample size is $n = 1000$ or larger, one cannot visually distinguish the two histograms from each other. This illustrates that for sample sizes $n = 1000$ or larger, the effect of the ICA step is close to negligible. Hereby, we have omitted the histograms corresponding to sample sizes $10^5, 10^6$ and 10^7 , as they carry no new information.

When comparing the performances of the Hill estimator and the moment estimator, Figure B5 indicates that the variance of the moment estimator is larger of the two. However, the moment estimates seem to be more evenly centered around the true γ . On the other hand, the Hill estimator seems to be slightly biased, as is expected De Haan and Ferreira (2007). The bias seems to decrease as the sample size increases. The results are thus overall largely similar to the time series example in the main text.

Figure B6 illustrates the absolute differences, scaled with $\sqrt{k_n}$, between

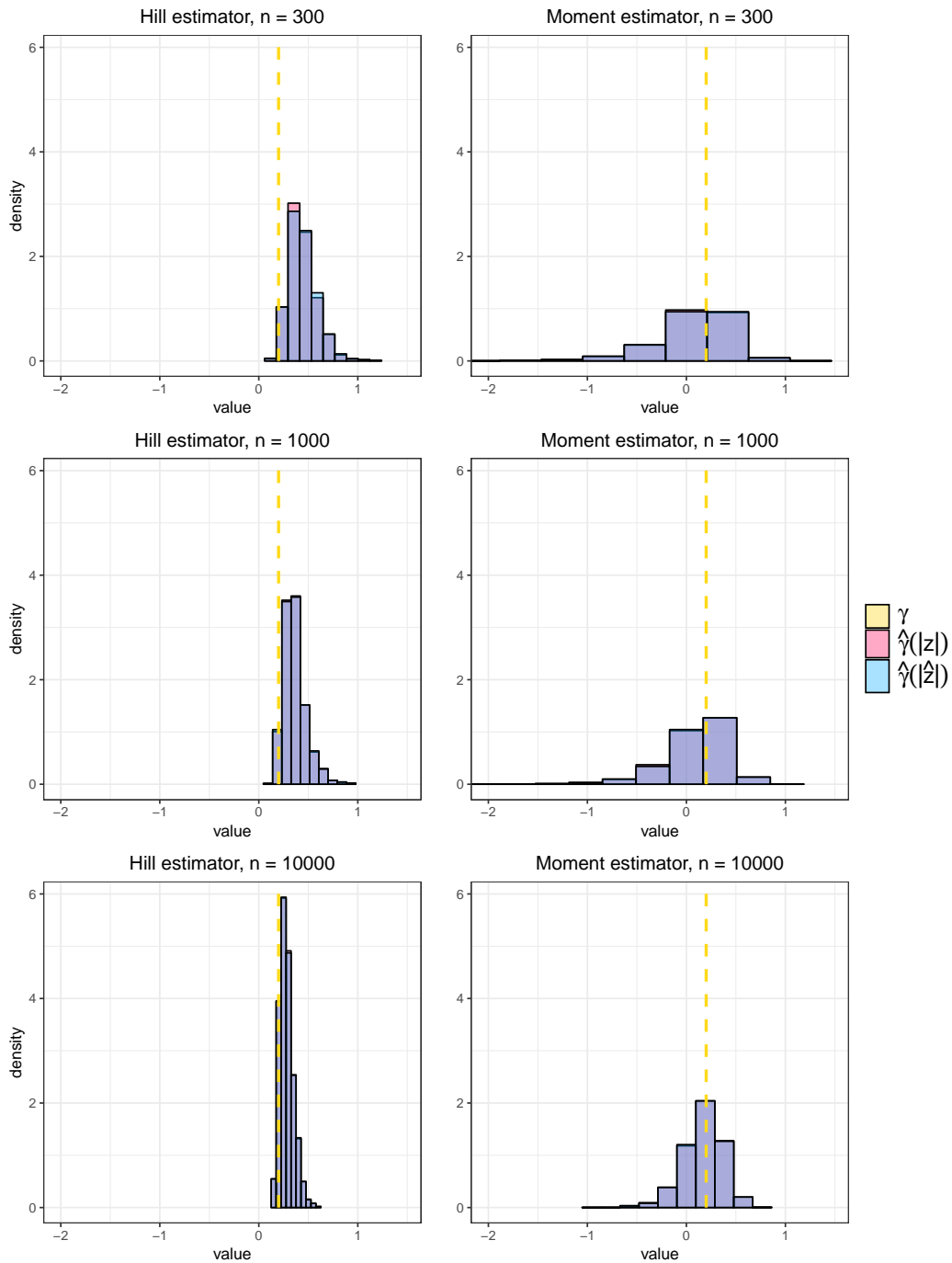


Figure B5: Histograms of $\hat{\gamma}(|z|)$ (light red) and $\hat{\gamma}(|\hat{z}|)$ (light blue) in the auxiliary simulation study with sample sizes 300, 1000 and 10 000. The dashed yellow vertical line is the theoretical extreme value index $\gamma = 1/5$. The dark blue color in the histograms represents the area, where the two histograms overlap.

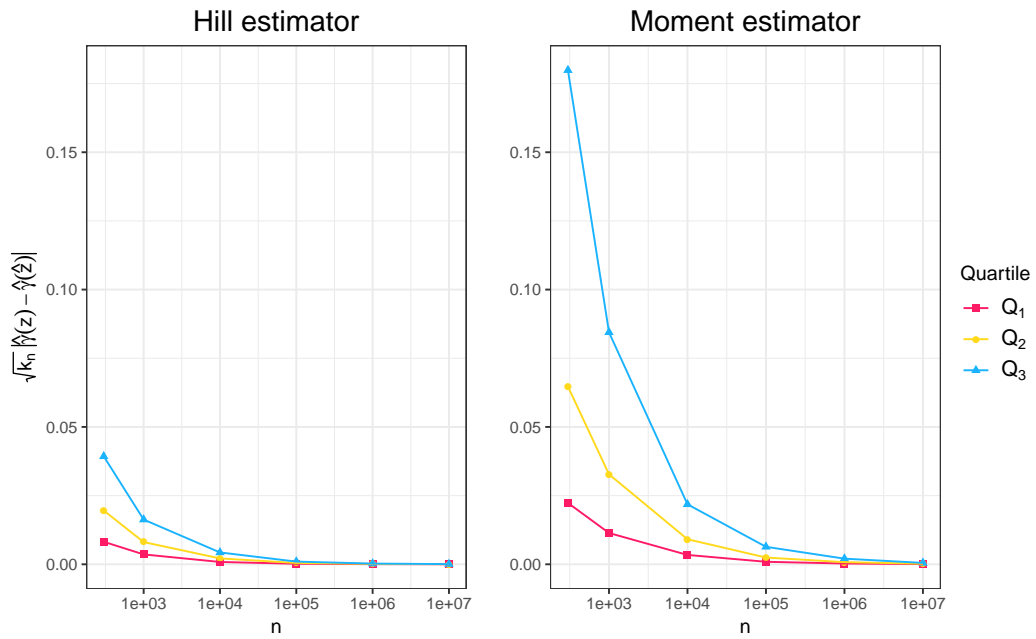


Figure B6: The quartiles of $\sqrt{k_n} |\hat{\gamma}(\mathbf{z}) - \hat{\gamma}(\hat{\mathbf{z}})|$ for the Hill estimator and the moment estimator in the auxiliary simulation study.

the extreme value index estimates calculated from $|\mathbf{z}|$ and $|\hat{\mathbf{z}}|$. In Figure B6, the red and blue curves represent the first and third empirical quartiles, respectively. Additionally, the yellow curve is the corresponding sample median curve. The differences seem to converge to zero for both the Hill and the moment estimator. However, the moment estimator seems to require larger sample sizes for the convergence. The quartile Q_3 that corresponds to the Hill estimator is close to zero with sample sizes larger or equal to 10^5 . Conversely, in this simulation study, the moment estimator quartile Q_3 requires samples of size 10^7 in order for it to be equally close to zero.

C Additional figures for the real data example

Figure C7 shows the original four-variate time series \mathbf{x}_i analysed in the real data example in Section 6 of the main text. Figure C8 shows the four latent series estimated from the four series in Figure C7 with generalized SOBI (Miettinen et al., 2019).

References

- Belouchrani, A., K. Abed-Meraim, J.-F. Cardoso, and E. Moulines (1997). A blind source separation technique using second-order statistics. *IEEE Transactions on Signal Processing* 45(2), 434–444.
- Bradley, R. (2005). Basic properties of strong mixing conditions. a survey and some open questions. *Probability Surveys* 2, 107–144.
- Cai, J.-J., J. H. Einmahl, L. De Haan, et al. (2011). Estimation of extreme risk regions under multivariate regular variation. *Annals of Statistics* 39(3), 1803–1826.
- Cardoso, J.-F. (1989). Source separation using higher order moments. In *1989 International Conference on Acoustics, Speech, and Signal Processing*, pp. 2109–2112. IEEE.
- Cardoso, J.-F. and A. Souloumiac (1993). Blind beamforming for non-Gaussian signals. In *IEE Proceedings F - Radar and Signal Processing*, Volume 140, pp. 362–370. IET.



Figure C7: The log-returns of the S&P500 index and the stock prices of CISCO Systems, Intel Corporation and Sprint Corporation in the period of January 3rd, 1991 – September 12th, 2019.

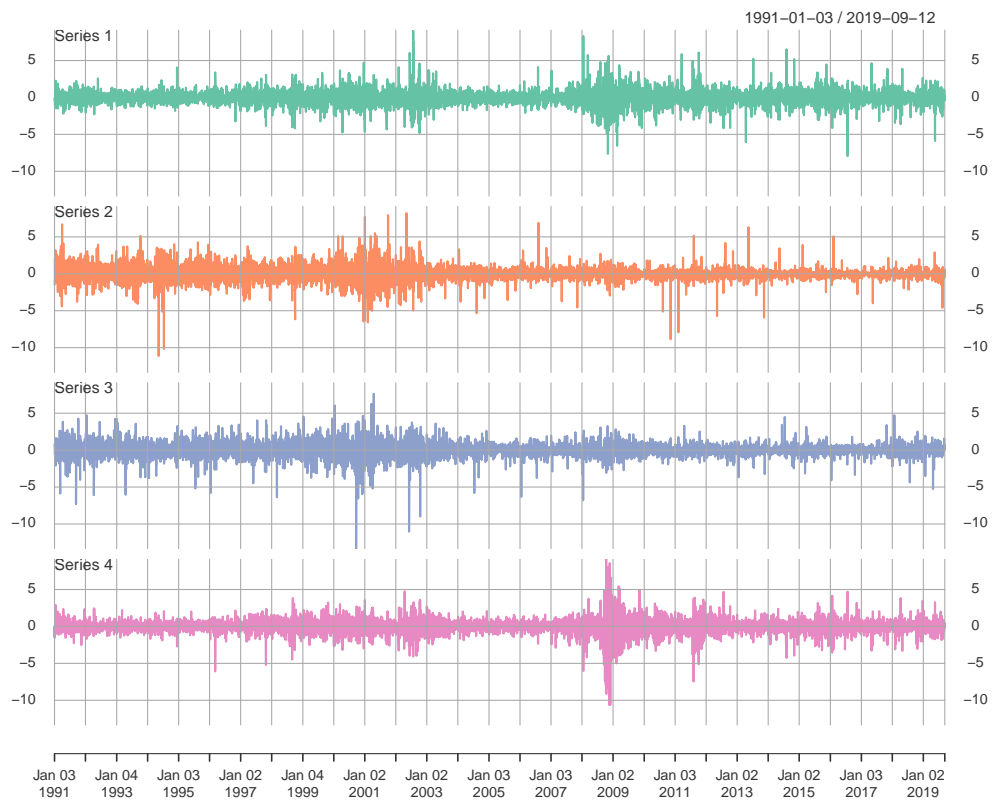


Figure C8: The latent source series estimated from the log-return observations with generalized SOBI.

- Comon, P. and C. Jutten (2010). *Handbook of Blind Source Separation: Independent Component Analysis and Applications*. Academic Press.
- De Haan, L. and A. Ferreira (2007). *Extreme Value Theory: an Introduction*. Springer Science & Business Media.
- De Haan, L., C. Mercadier, and C. Zhou (2016). Adapting extreme value statistics to financial time series: dealing with bias and serial dependence. *Finance and Stochastics* 20(2), 321–354.
- Dekkers, A. L., J. H. Einmahl, and L. De Haan (1989). A moment estimator for the index of an extreme-value distribution. *Annals of Statistics* 17(4), 1833–1855.
- Dematteo, A. and S. Cléménçon (2016). On tail index estimation based on multivariate data. *Journal of Nonparametric Statistics* 28(1), 152–176.
- Dominicy, Y., P. Ilmonen, and D. Veredas (2017). Multivariate Hill estimators. *International Statistical Review* 85(1), 108–142.
- Drees, H. (2000). Weighted approximations of tail processes for β -mixing random variables. *Annals of Applied Probability* 10(4), 1274–1301.
- Drees, H. (2002). Tail empirical processes under mixing conditions. In *Empirical process techniques for dependent data*, pp. 325–342. Boston: Birkhäuser Boston.
- Drees, H. (2003). Extreme quantile estimation for dependent data, with applications to finance. *Bernoulli* 9(4), 617–657.
- Embrechts, P., C. Klüppelberg, and T. Mikosch (2013). *Modelling Extremal Events: for Insurance and Finance*, Volume 33. Springer Science & Business Media.
- Fan, J., M. Wang, and Q. Yao (2008). Modelling multivariate volatilities via conditionally uncorrelated components. *Journal of the Royal Statistical Society: Series B (Statistical Methodology)* 70(4), 679–702.
- Heikkilä, M., Y. Dominicy, and P. Ilmonen (2019). On multivariate separating Hill estimator under estimated location and scatter. *Statistics* 53(2), 301–320.

- Hill, B. M. (1975). A simple general approach to inference about the tail of a distribution. *Annals of Statistics* 3(5), 1163–1174.
- Horn, R. A. and C. R. Johnson (1990). *Matrix Analysis*. Cambridge University Press.
- Hsing, T. (1991). On tail index estimation using dependent data. *Annals of Statistics* 19(3), 1547–1569.
- Hyvärinen, A. (1999). Fast and robust fixed-point algorithms for independent component analysis. *IEEE Transactions on Neural Networks* 10(3), 626–634.
- Hyvärinen, A. and E. Oja (2000). Independent component analysis: algorithms and applications. *Neural Networks* 13(4-5), 411–430.
- Ilmonen, P., J. Nevalainen, and H. Oja (2010). Characteristics of multivariate distributions and the invariant coordinate system. *Statistics & Probability Letters* 80(23), 1844–1853.
- Kim, M. and S. Lee (2017). Estimation of the tail exponent of multivariate regular variation. *Annals of the Institute of Statistical Mathematics* 69(5), 945–968.
- Kiviluoto, K. and E. Oja (1998). Independent component analysis for parallel financial time series. In *ICONIP*, Volume 2, pp. 895–898.
- Lietzén, N., L. Viitasaari, and P. Ilmonen (2020). Modeling temporally uncorrelated components for complex-valued stationary processes. arXiv preprint arXiv:2003.04199.
- Lu, C.-J., T.-S. Lee, and C.-C. Chiu (2009). Financial time series forecasting using independent component analysis and support vector regression. *Decision Support Systems* 47(2), 115–125.
- Miettinen, J., K. Illner, K. Nordhausen, H. Oja, S. Taskinen, and F. J. Theis (2016). Separation of uncorrelated stationary time series using autocovariance matrices. *Journal of Time Series Analysis* 37(3), 337–354.
- Miettinen, J., M. Matilainen, K. Nordhausen, and S. Taskinen (2019). Extracting conditionally heteroskedastic components using independent component analysis. *Journal of Time Series Analysis*.

- Miettinen, J., K. Nordhausen, H. Oja, and S. Taskinen (2017). *fICA: Classical, Reloaded and Adaptive FastICA Algorithms*. R package version 1.1-0.
- Miettinen, J., K. Nordhausen, H. Oja, S. Taskinen, and J. Virta (2017). The squared symmetric FastICA estimator. *Signal Processing* 131, 402–411.
- Miettinen, J., K. Nordhausen, and S. Taskinen (2017). Blind source separation based on joint diagonalization in R: The packages JADE and BSSasyp. *Journal of Statistical Software* 76(2), 1–31.
- Miettinen, J., S. Taskinen, K. Nordhausen, and H. Oja (2015). Fourth moments and independent component analysis. *Statistical Science* 30(3), 372–390.
- Nordhausen, K., H. Oja, and E. Ollila (2008). Robust independent component analysis based on two scatter matrices. *Austrian Journal of Statistics* 37(1), 91–100.
- Nualart, D. (2006). Fractional Brownian motion: stochastic calculus and applications. In *International Congress of Mathematicians*, Volume 3, pp. 1541–1562. European Mathematical Society.
- Oja, H., S. Sirkiä, and J. Eriksson (2006). Scatter matrices and independent component analysis. *Austrian Journal of Statistics* 35(2&3), 175–189.
- Rachev, S. T. (2003). *Handbook of Heavy Tailed Distributions in Finance: Handbooks in Finance*. Elsevier.
- Resnick, S. and C. Stărică (1997). Asymptotic behavior of Hill’s estimator for autoregressive data. *Communications in Statistics. Stochastic Models* 13(4), 703–721.
- Roberts, S. J. (2000). Extreme value statistics for novelty detection in biomedical data processing. *IEE Proceedings-Science, Measurement and Technology* 147(6), 363–367.
- Rootzén, H. (1995). The tail empirical process for stationary sequence. Preprint, Chalmers University, Gothenburg.
- Rootzén, H. (2009). Weak convergence of the tail empirical function for dependent sequences. *Stoch. Proc. Appl.* 119(2), 468–490.

- Smith, M., S. Reece, S. Roberts, and I. Rezek (2012). Online maritime abnormality detection using Gaussian processes and extreme value theory. In *2012 IEEE 12th International Conference on Data Mining*, pp. 645–654. IEEE.
- Stărică, C. (1999). On the tail empirical process of solutions of stochastic difference equations. Preprint, Chalmers University, Gothenburg.
- Tong, L., R.-W. Liu, V. C. Soon, and Y.-F. Huang (1991). Indeterminacy and identifiability of blind identification. *IEEE Transactions on circuits and systems* 38(5), 499–509.
- Tong, L., V. Soon, Y. Huang, and R. Liu (1990). AMUSE: a new blind identification algorithm. In *Proceedings of IEEE International Symposium on Circuits and Systems*, pp. 1784–1787.
- Yang, S. and Z. Yi (2005). Fast ICA for online cashflow analysis. In *International Symposium on Neural Networks*, pp. 891–896. Springer.